

# Sketchy: Memory-efficient Adaptive Regularization with Frequent Directions

Vladimir Feinberg<sup>1</sup> Xinyi Chen<sup>1,2</sup> Y. Jennifer Sun<sup>2</sup> Rohan Anil<sup>1</sup> Elad Hazan<sup>1,2</sup>

## Abstract

Adaptive regularization methods that exploit more than the diagonal entries exhibit state of the art performance for many tasks, but can be prohibitive in terms of memory and running time. We find the spectra of the Kronecker-factored gradient covariance matrix in deep learning (DL) training tasks are concentrated on a small leading eigenspace that changes throughout training, motivating a low-rank sketching approach. We describe a generic method for reducing memory and compute requirements of maintaining a matrix preconditioner using the Frequent Directions (FD) sketch. Our technique allows interpolation between resource requirements and the degradation in regret guarantees with rank  $k$ : in the online convex optimization (OCO) setting over dimension  $d$ , we match full-matrix  $d^2$  memory regret using only  $dk$  memory up to additive error in the bottom  $d - k$  eigenvalues of the gradient covariance. Further, we show extensions of our work to Shampoo, placing the method on the memory-quality Pareto frontier of several large scale benchmarks.

## 1. Introduction

DL optimization commonly relies on adaptive gradient methods, namely the Adam optimizer (Kingma & Ba, 2015). It differs from stochastic gradient descent in that the learning rate is a structured diagonal matrix built from previous gradients rather than a scalar. In full matrix AdaGrad (Duchi et al., 2011) the inverse matrix square root of the sum of outer products of previous gradients is the learning rate.

Full matrix preconditioning is impractical for modern deep learning architectures: for instance, the ResNet-50 architecture (He et al., 2016) has over 23 million parameters, requiring more than 2 petabytes to represent its gradient covariance. Thus, diagonal preconditioning methods remain

<sup>1</sup>Google Research, Brain Team <sup>2</sup>Princeton University. Correspondence to: Vladimir Feinberg <vladf@google.com>.

Preliminary work.

popular. However, previous work has demonstrated state-of-the-art results in some settings, such as large-batch data parallel training, for nondiagonal forms of preconditioning (Martens & Grosse, 2015; Gupta et al., 2018; Agarwal et al., 2019; Chen et al., 2019; Anil et al., 2019; 2020). Furthermore, as hardware evolves, memory efficiency becomes an increasing concern, as “logic improves much faster than wires and SRAM, so logic is relatively free” (Jouppi et al., 2021): from TPUv2 to TPUv3, per-chip bfloat16 operations per second improved  $2.67\times$  but memory bandwidth only improved  $1.29\times$ . GPUs exhibit a similar pattern for compute and memory increase, at  $5\times$  and  $2.2\times$ , for V100 to A100 (Dally et al., 2021).

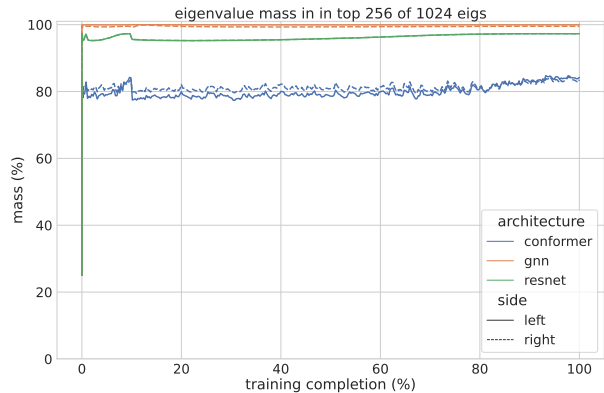


Figure 1: Low-rank nuclear norm relative error. We tune ResNet-50, a Conformer, and a Graph Neural Net (GNN), with Shampoo across three different datasets (see Sec. 5.1). For a 2D layer with gradients  $G$ , Shampoo tracks the exponential moving average of factors  $GG^\top$  and  $G^\top G$  (left and right sides). We select a  $1024 \times 1024$  covariance factor  $C$  across all these architectures for both sides and plot the proportion of spectral mass captured by the top 256 eigenvalues, i.e.,  $\sum_{i=1}^{256} \lambda_i(C) / \sum_{i=1}^{1024} \lambda_i(C)$ .

Spectral investigation into the Kronecker-factored gradient covariance matrix reveals a concentrated, but changing, spectrum (Fig. 1), suggesting the majority of the spectral mass can be represented by a low-rank matrix, albeit rotating over time. The Frequent Directions (FD) sketch provides a mechanism to track the top eigenvectors without materializing the full covariance matrix (Ghashami et al., 2016).

Is a large portion of the spectral mass sufficient to retain the performance of adaptive regularization in theory and practice? We investigate this hypothesis.

In this work, we demonstrate:

- In the setting of online convex optimization, by applying a dynamic diagonal regularization to the FD sketch, we can recover full-matrix AdaGrad regret up to additive spectral terms under a memory constraint, providing a novel guarantee without curvature assumptions (Sec. 4.1). We show how to rigorously compose our approach with Shampoo (Sec. 4.2).
- The moving average of Kronecker-factored gradient covariance exhibits fast spectral decay in practical DL settings (Sec. 5.1); these correspond to precisely the matrices we must sketch with Shampoo.
- By modifying FD to be compatible with exponential moving averages (Sec. 4.3), we develop a practical algorithm which approximately recovers Shampoo performance in three modern DL settings (ImageNet image classification, LibriSpeech audio transcription, and ogbg-molpcba molecule structure identification) (Sec. 5.2, 5.3).

## 2. Related Work

### 2.1. Spectral Analysis of DL Training

Denote the loss function of the  $i$ -th example for weights  $x$  as  $f_i(x)$ . The spectrum of the Hessian matrix  $\sum_i \nabla^2 f_i$  has been the subject of intensive investigation in DL (Sagun et al., 2016; 2017; Ghorbani et al., 2019; Sankar et al., 2021) and its properties have been used to devise training methods (Martens & Grosse, 2015; Agarwal et al., 2017).

Recent papers (Gur-Ari et al., 2018; Bakker et al., 2018; Xie et al., 2022) inspect the covariance matrix,  $\sum_i (\nabla f_i)(\nabla f_i)^\top$ . In small models, where its computation is feasible, these works identify fast spectral decay.

Agarwal et al. (2019) take advantage of this observation by using a low-rank approximation of the whole covariance matrix, based on a limited history of the gradients,  $\sum_{i=t-r}^r (\nabla f_i)(\nabla f_i)^\top$ . This approach still requires  $r$  copies of the model gradients in memory, where typically  $r$  should scale with  $\beta_2^{-1}$ , with  $\beta_2$  the exponential moving average for second order statistics (the authors set  $r = 200$ ). Fundamentally, approximating the whole covariance matrix constrains Agarwal et al. (2019) application to small models.

In our work, we validate the decay hypothesis holds across the per-layer factored covariance matrices in several modern neural networks. For a layer’s gradient matrix  $G_i$  at the  $i$ -th example and a second moment decay term  $\beta_2$ , our

work inspects spectral decay for  $L_t = \sum_i \beta_2^{t-i} G_i G_i^\top$  and  $R_t = \sum_i \beta_2^{t-i} G_i^\top G_i$ ; the spectral structure for these outer products is not well-documented. Furthermore, as described in Sec. 2.4, approximating the factored covariance  $L_t \otimes R_t$  requires less memory than the full covariance and explains why our method can scale to large modern architectures whereas Agarwal et al. (2019) cannot.

### 2.2. Sublinear Memory Methods

Extreme Tensoring (Chen et al., 2019), AdaFactor (Shazeer & Stern, 2018), and SM3 (Anil et al., 2019) are methods that require sublinear memory relative to the number of parameters, at the other end of the memory-quality tradeoff beyond methods that rely on the diagonal of the gradient covariance such as Adam. Owing to different structural assumptions on the set of feasible preconditioners, comparison with these methods is out of scope. However, these methods may compose with our approach. One may apply Extreme Tensoring first, then sketch the resulting reshaped tensor covariances with our method to further reduce memory consumption.

### 2.3. Sketching-based Approaches

Several works have explored sketching-like approximations to the gradient covariance matrix, but none provide an adaptive bound exploiting fast spectral decay in gradient covariance without additional assumptions (Tbl. 1). In this section, we consider the OCO setting over dimension  $d$  (Sec. 3).

Random projection (Ada-LR) is most spiritually similar to our work (Krummenacher et al., 2016). Although it does not reduce memory usage, it relies on random projections to lower dimension  $\ell \leq d$  to reduce inverse matrix computation costs. A heuristic alternative, RadaGrad, is also proposed, which reduces memory consumption to  $O(d\ell)$ , similar to our rigorous approach. However, as with all Johnson-Lindenstrauss projection methods, it suffers a failure rate scaling as  $O(\ell^{-1})$  (in comparison, our method inherits FD’s determinism).

Frequent Directions (FD) (Ghashami et al., 2016; Liberty, 2022), provides an alternative matrix sketching approach from the data streaming literature. As an adaptive sketch, it dominates random projection in terms of matrix recovery, and lower bounds show its memory usage is optimal up to universal multiplicative constants.

In the context of exp-concave cost functions, Luo et al. (2016) provide an FD sketched version of Online Newton Step (ONS), FD-SON. In this setting, their approach nearly recovers classical ONS regret, up to logarithmic error in  $\sum_{i=1}^{\ell-1} \lambda_i(G_T)$  and additive error in  $\sum_{i=\ell}^d \lambda_i(G_T)$ . However, without the exp-concave assumption, FD-SON falls back to a gradient-descent-like default regret of  $O(\sqrt{T})$ .

Table 1: Memory-efficient adaptive gradient methods, in the OCO setting with dimension  $d$  (Sec. 3). We describe the worst-case regret bounds without exp-concavity assumptions, asymptotically, hiding logarithmic factors, treating the decision set diameter as a constant, and assume optimally-tuned hyperparameters.  $\ell$  refers to the controllable preconditioner rank. Note  $\text{tr } G_T^{1/2} = \sqrt{\min_{H \in \mathcal{H}} \sum_t \|\nabla_t\|_H^2}$  is the optimal preconditioner's regret among the class of positive semi-definite, unit-trace matrices,  $\mathcal{H}$ , and  $G_T$  is the sum of gradient outer products. We let eigenvalues  $\lambda_i = \lambda_i(G_T)$  with  $\lambda_{i:j} = \sum_{m=i}^j \lambda_m$ .

Reference	Regret (general convex)	Memory
Full Matrix AdaGrad (Duchi et al., 2011)	$\text{tr } G_T^{1/2}$	$d^2$
Ada-LR (Krummenacher et al., 2016)	$\text{tr } G_T^{1/2} + \lambda_{\ell+1}^{1/2} \ell^{3/4} d^{1/4}$	$d^2$
Ada-FD (Wan & Zhang, 2021)	$\Omega(T^{3/4})^1$	$d\ell$
SON (Luo et al., 2016)	$\sqrt{Td}$	$d^2$
FD-SON (Luo et al., 2016)	$\sqrt{\ell \lambda_{\ell:d} T}$	$d\ell$
This paper	$\text{tr}(G_T^{1/2}) + \sqrt{d(d-\ell)\lambda_{\ell:d}}$	$d\ell$

Wan & Zhang (2021) extend the FD-SON approach to the AdaGrad setting, by adding a fixed diagonal perturbation  $\delta I$  to an FD-based preconditioner, in Ada-FD. However, this approach does not achieve  $\sqrt{T}$  regret even in a non-adversarial setting with stochastic linear cost functions (Observation 1), where learning rate and  $\delta$  are tuned. Dynamically changing diagonal regularization is essential for worst-case  $O(\sqrt{T})$  performance.

**Observation 1.** Suppose we receive linear cost functions  $f_t(x) = \langle x, g_t \rangle$ , where  $g_t \in \mathbb{R}^d$  is a random vector drawn iid from any distribution over  $r \leq d$  orthonormal vectors  $W$ . For any sketch size  $\ell \leq r$ , the bound on the expected regret of Ada-FD is  $\Omega(T^{3/4})$ .

Wan & Zhang (2021) remark Ada-FD has  $\sqrt{T}$  regret when  $G_T$  is low rank with rank below  $k$ , so  $d - k$  of its eigenvalues are precisely zero. However, this setting does not require any sketching in the first place. By tracking the column space of observed gradients (e.g., with a reduced QR decomposition, rank-1-updated every step), the full matrix AdaGrad algorithm can be perfectly recovered without using more than  $O(dk)$  memory.

#### 2.4. Shampoo

Perhaps our most compelling application is reducing the memory of Shampoo (Gupta et al., 2018; Anil et al., 2020). Table 2 elaborates why the composition of FD and Shampoo is essential to avoid memory consumption asymptotically greater than parameter count for approximate full matrix regularization.

However, Shampoo memory costs may still be prohibitive for rectangular weight matrices. An  $n \times m$  weight matrix  $W$  will have left and right preconditioners  $L, R$  in Shampoo of size  $n \times n$  and  $m \times m$ , respectively, with the preconditioning operation  $(L \otimes R)\vec{\text{vec}}(W) = \vec{\text{vec}}(LWR)$ . In BERT-Large (Devlin et al., 2019), most parameters are in the feed-

forward network layers, which consist of  $4096 \times 1024$  dense kernels; other transformers follow similar narrow-to-wide patterns. For large models, occupying even  $4 \times$  memory for the left preconditioner can frequently result in OOM in memory-constrained settings; this was in fact one of the practical motivations for our proposed approach.

Table 2: Asymptotic memory consumption of super-diagonal adaptive regularization approaches for a single matrix parameter of size  $n \times m$ . Here,  $r$  refers to the GGT history buffer and  $k$  to the approximation rank of FD (both typically set to hundreds). GGT requires superlinear memory (a multiple of  $r$ ) and Shampoo does too (e.g., if  $m/n$  is large). We excerpt an additive  $O(mn)$  factor present in all implementations for momentum terms and the size of the parameters themselves. Blocked Shampoo composes with our approach, though asymptotically blocking is unnecessary as  $k \leq \min(m, n)$ ; see discussion in Sec. 2.4.

Reference	Memory
GGT (Agarwal et al., 2019)	$mnr$
Shampoo (Gupta et al., 2018)	$m^2 + n^2$
Blocked Shampoo (Anil et al., 2020)	$mn$
This paper	$mk + nk$

Anil et al. (2020) introduces two workarounds for the problem of rectangular matrices based on limiting covariance modelling. Furthermore, both approximations can be applied to our method, so we do not compare against them. First, the authors propose Blocked Shampoo, which views each weight matrix  $W$  of shape  $m \times n$  as  $mn/b^2$  blocks of size  $b \times b$  for some block size  $b < \min(m, n)$  (in the limit

<sup>1</sup>The regret of Ada-FD is expressed in terms of dynamic runtime quantities which do not admit a universal bound in terms of  $G_T$ ; we display its regret for the specific case of Observation 1 instead (a detailed look at its regret is given in Appendix A.1).

$b = 1$ , this recovers diagonal AdaGrad). This approach is dependent on the ordering of neurons in hidden layers. Another approximation relies on only one-sided covariance upper bounds,  $L_t \otimes I$  or  $I \otimes R_t$ . Note, however, that the one-sided approximation doesn't help with vector parameters, such as those that appear for the bias terms in dense layers or layer norms (Ba et al., 2016). For 3D weights, such as those which appear in homogeneous Mixtures of Experts (Shazeer et al., 2017), blocking increases memory consumption.

### 3. Setting and Definitions

**Regret and Optimization.** The optimization problem of training a deep neural network has a non-convex objective loss function  $f$ . Since finding the global optimum is computationally intractable in general, theoretical guarantees focus on convergence to an  $\varepsilon$ -approximate first-order optimum: a point  $x$  such that  $\|\nabla f(x)\| \leq \varepsilon$ . The analysis of stochastic subgradient methods for smooth non-convex optimization is particularly simple, see e.g. (Bubeck et al., 2015; Hazan, 2019).

Adaptive gradient methods, that are state of the art in deep learning training, are more sophisticated to analyze. They use a matrix preconditioner and derive their theoretical results from the theory of regret minimization in online convex optimization (OCO) (Hazan et al., 2016). In the OCO setting, a learner chooses a point  $x_t \in \mathcal{K}$  iteratively, where  $\mathcal{K} \subseteq \mathbb{R}^d$  is a convex decision set (take  $\mathcal{K} = \mathbb{R}^d$  if unconstrained). After the decision is made, the adversary reveals a convex loss function  $f_t$ , to which the algorithm suffers cost  $f_t(x_t)$ . Upon receiving the cost, the algorithm updates its decision for the next iteration.

The regret suffered by the algorithm in time horizon  $T$  is defined to be the excess of loss actually suffered by the algorithm's decisions than the single best decision point in  $\mathcal{K}$  provided hindsight of  $f_1, \dots, f_T$ . Formally, the regret for an online algorithm  $\mathcal{A}$  is given by

$$\text{Regret}_T^{\mathcal{A}} = \sum_{t=1}^T f_t(x_t) - \min_{x \in \mathcal{K}} \sum_{t=1}^T f_t(x) ,$$

where  $x_1, \dots, x_T$  are the decisions played by the algorithm.

A smooth non-convex optimization can be reduced to solving a series of offline convex problems (Agarwal et al., 2019). The convex sub-problems have form

$$f_t(x) = f(x) + c\|x - x_t\|^2 ,$$

where  $c$  is a constant and  $x_t$  is an iterate in the optimization process. Using online-to-batch conversion, we can translate the regret bound of an OCO algorithm to convergence guarantees for offline optimization. Therefore, non-convex

optimization guarantees can be obtained from regret bounds, and we focus on the latter in this paper.

**Sketching and the Frequent Directions Method.** Given a stream of vectors  $g_t \in \mathbb{R}^d$ ,  $t \in [T]$ , we utilize the FD sketch (Ghashami et al., 2016) which maintains a low-rank approximation of the true running covariance  $G_t = \sum_{s \leq t} g_s g_s^\top$ .

At each time  $t$ , maintains a matrix  $B_t$  of size  $d \times \ell$  whose last column is 0 and whose square is  $B_t B_t^\top = \tilde{C}_t$ . After seeing  $g_t$  from the stream, we update the previous matrix using Alg. 1, which outputs  $B_{t+1}$  of size  $d \times \ell$  whose last column remains 0; take  $B_0 = 0$ . At every iteration  $t$ , denote  $\rho_t := \lambda_\ell^{(t)}$  be the removed eigenvalue from the covariance update in Alg. 1.

For convenience, let  $\rho_{1:t} \stackrel{\text{def}}{=} \sum_{s=1}^t \rho_s$ . For a matrix  $X$ , we denote its  $i$ -th leading eigenvalue by  $\lambda_i(X)$ . Let  $\|\cdot\|_F$  denote the Frobenius norm of a matrix.

### 4. Algorithms and Main Theorems

In this section, we introduce the adaptation of Frequent Directions (FD) to AdaGrad (Sec. 4.1) and Shampoo (Sec. 4.2), the corresponding algorithms and regret guarantees. Additionally, in Sec. 4.3, we modify FD to support exponential moving averages. We start with FD, Alg. 1 from Liberty (2022).

---

#### Algorithm 1 Frequent Directions Update (FD-update)

**Require:** Invariant that last column of  $B_{t-1}$  is 0.

**Ensure:** The last column of  $B_t$  is 0.

- 1: Input: Previous state  $\tilde{G}_{t-1} = B_{t-1} B_{t-1}^\top \in \mathbb{R}^{d \times d}$
- 2: Input: New symmetric PSD matrix  $M_t \in \mathbb{R}^{d \times d}$ .
- 3: Eigendecompose  $\tilde{U}_t \text{ diag } \lambda^{(t)} \tilde{U}_t^\top = \tilde{G}_{t-1} + M_t$  where  $\lambda^{(t)}$  is a vector with the eigenvalues in descending order.
- 4: Define  $U_t$  as the matrix whose columns are the first  $\ell$  columns of  $\tilde{U}_t$ , and  $\lambda_{[1:\ell]}^{(t)}$  be its eigenvalues.
- 5: Update  $B_t = U_t \text{ diag } \left( \lambda_{[1:\ell]}^{(t)} - \lambda_\ell^{(t)} \right)^{1/2}$ .

**output**  $\lambda_\ell^{(t)}, B_t B_t^\top$ .

---

The fundamental property of FD is that applying Alg. 1 over a stream of vectors  $g_t$ , with  $B_0 = 0$ , the sum of escaped mass  $\rho_t = \lambda_\ell^{(t)}$  can be limited by spectra of  $G_T$ .

**Lemma 2.** *The quantity  $\rho_{1:T}$  can be upper bounded as*

$$\rho_{1:T} \leq \min_{k=0, \dots, \ell-1} \frac{\sum_{i=k+1}^d \lambda_i(G_T)}{\ell - k} \leq \sum_{i=\ell}^d \lambda_i(G_T) .$$

#### 4.1. FD for AdaGrad

Our main algorithm in this section is Alg. 2 run with FD (Alg. 1) as the sketching method.  $\tilde{G}_t^{-1/2}$  in Alg. 2 denotes the Moore-Penrose pseudoinverse of the matrix  $\tilde{G}_t^{1/2}$ .

#### Algorithm 2 Sketchy AdaGrad (S-AdaGrad)

---

```

1: Input: constraint set  $\mathcal{K}$ , step size  $\eta$ , time horizon  $T$ , covariance-sketching algorithm  $\mathcal{A}$ .
2: Initialize  $x_1 \in \mathcal{K}$ ,  $\tilde{G}_0 = \tilde{G}_0 = 0$ .
3: for  $t = 1, \dots, T$  do
4:   Play  $x_t$ , receive  $g_t \in \partial f_t(x_t)$ , suffer cost  $f_t(x_t)$ .
5:   Sketch  $(\rho_t^L, \tilde{G}_t) = \mathcal{A}(\tilde{G}_{t-1}, g_t g_t^\top)$ .
6:   Update  $\tilde{G}_t = \tilde{G}_t + \rho_{1:t} I$ .
7:   Update  $y_{t+1} = x_t - \eta \tilde{G}_t^{-1/2} g_t$ .
8:   Update  $x_{t+1} = \operatorname{argmin}_{x \in \mathcal{K}} \|y_{t+1} - x\|_{\tilde{G}_t^{1/2}}^2$ .
9: end for

```

---

**Theorem 3.** Suppose Alg. 2 is run with subroutine  $\mathcal{A}$  taken to be FD-update (Algorithm 1). Define  $\Omega_\ell = \min_{k < \ell} (\ell - k)^{-1} \sum_{i=k+1}^d \lambda_i(G_T)$ , then with  $\eta = \frac{D}{\sqrt{2}}$ , Alg. 2 guarantees the following additive regret bound:

$$\text{Regret}_T(\text{S-AdaGrad}) \leq D \left( \sqrt{2} \operatorname{tr} G_T^{1/2} + d \sqrt{\frac{\Omega_\ell}{2}} \right),$$

where  $D$  is taken to be diameter of the constraint set  $\mathcal{K}$  if  $\mathcal{K}$  is bounded and  $\max_{t \in [T]} \|x_t - x^*\|_2$  otherwise.

Notably in Theorem 3,  $\text{Regret}_T = O(\sqrt{T})$  always and the dependence  $\Omega_\ell$  on lower eigenvalues of  $G_T$  is additive.

**Corollary 4.** We can improve Theorem 3 slightly to

$$\text{Regret}_T \leq D \left( \sqrt{2} \operatorname{tr} G_T^{1/2} + \sqrt{\frac{d(d-\ell)\Omega_\ell}{2}} \right).$$

The regret bound above holds under the optimal tuning of the learning rate, which depends on problem quantities that can be unknown a priori. It is possible to design a parameter-free variant of Alg. 2 by using  $\|x\|_t^2 = x^\top (\tilde{G}_t + I)^{1/2} x$  as the norms  $\|\cdot\|_t$  in Cutkosky (2020).

#### 4.2. FD for Shampoo

In this section, we adapt FD-update to Shampoo (Gupta et al., 2018). For simplicity, we optimize over  $\mathbb{R}^{m \times n}$  in Alg. 3; projection may be handled as in Alg. 2.

Denote

$$L_T \stackrel{\text{def}}{=} \sum_{t=1}^T G_t G_t^\top + \varepsilon I, \quad R_T \stackrel{\text{def}}{=} \sum_{t=1}^T G_t^\top G_t + \varepsilon I.$$

#### Algorithm 3 Sketchy Shampoo (S-Shampoo)

---

```

1: Input:  $\eta, T$ , sketching algorithm  $\mathcal{A}$ .
2: Initialize  $X_0 = 0_{m \times n}$ ,  $\tilde{L}_0 = \varepsilon I_m$ ,  $\tilde{R}_0 = \varepsilon I_n$ ,  $\bar{L}_0 = 0_m$ ,  $\bar{R}_0 = 0_n$ .
3: for  $t = 1, \dots, T$  do
4:   Play  $X_t$ , suffer  $f_t(X_t)$ , receive  $G_t \in \partial f_t(X_t)$ .
5:   Sketch  $(\rho_t^L, \tilde{L}_t) = \mathcal{A}(\bar{L}_{t-1}, G_t G_t^\top)$ ,  $(\rho_t^R, \tilde{R}_t) = \mathcal{A}(\bar{R}_{t-1}, G_t^\top G_t)$ .
6:   Update  $\bar{L}_t = \bar{L}_{t-1} + \rho_{1:t}^L I_m$ ,  $\tilde{R}_t = \bar{R}_{t-1} + \rho_{1:t}^R I_n$ .
7:   Update  $X_{t+1} = X_t - \eta \tilde{L}_t^{-1/4} G_t \tilde{R}_t^{-1/4}$ .
8: end for

```

---

**Theorem 5.** Suppose  $G_1, \dots, G_T$  have rank at most  $r$ . Then Alg. 3 run with subroutine  $\mathcal{A}$  taken to be FD-update (Alg. 1) and  $\eta = D/\sqrt{2r}$  guarantees that  $\text{Regret}_T(\text{S-Shampoo})$  is bounded above by

$$\sqrt{2r}D \left( \operatorname{tr}(L_T^{1/4}) + m\Omega_{L,\ell}^{1/4} \right) \left( \operatorname{tr}(R_T^{1/4}) + n\Omega_{R,\ell}^{1/4} \right),$$

where  $D = \max_{t \in [T]} \|X_t - X^*\|_F$  and  $\Omega_{L,\ell}, \Omega_{R,\ell}$  are analogous bounds for  $\rho_{1:T}^L, \rho_{1:T}^R$  from Lem. 2.

We can derive a slightly better bound analogous to Cor. 4 for Alg. 3, but we omit the similar proof due to space limits.

#### 4.3. Exponentially Weighted FD

This section discusses a modification to the FD-update routine (Alg. 1) to support exponential moving averages.

Early in algorithm development, we noticed that attempting to approximate the unweighted sum of factored gradient covariances  $\sum_t G_t G_t^\top$  and  $\sum_t G_t^\top G_t$  with FD tended to an estimate of covariance that was roughly 0, creating numerical instabilities. Note that the FD guarantee (Lem. 2) still holds—but the error term  $\rho_{1:T}$  becomes greater than  $\|G_T\|$ , which results in a vacuous bound due to lack of spectral decay.

Indeed, Fig. 1 motivating this work only confirmed that the exponential moving average  $L_t(\beta_2) = \sum_t \beta_2^{T-t} G_t G_t^\top$  exhibits fast spectral decay (and analogously for  $R_t$ ). Luckily, thanks to the recursion  $L_{t+1}(\beta_2) = \beta_2 L_t + G_{t+1} G_{t+1}^\top$ , the FD sketch may easily be adopted for this setting.

**Observation 6.** Given a stream  $g_t$  of vectors for  $t \in [T]$ , sketch size  $\ell$ , and updates  $(\rho_t^{(\beta_2)}, \tilde{G}_t^{(\beta_2)}) = \text{FD-update}(\beta_2 \tilde{G}_{t-1}^{(\beta_2)}, g_t g_t^\top)$ , then we have

$$\left\| \tilde{G}_T^{(\beta_2)} - G_T^{(\beta_2)} \right\| \leq \rho_{1:T}^{(\beta_2)} \leq \min_{k < \ell} \frac{\sum_{i=k+1}^d \lambda_i(G_T^{(\beta_2)})}{\ell - k},$$

where  $G_T^{(\beta_2)} = \sum_{t=1}^T \beta_2^{T-t} g_t g_t^\top$ .

## 5. Experiments

We investigate the following empirical questions.

- Does the factored gradient covariance exhibit fast spectral decay amenable to FD sketching? (Sec. 5.1)
- How much of Shampoo’s quality can our low-memory approach recover? (Sec. 5.2)
- Can we explain generalization improvement through better optimization? (Sec. 5.3)

For repeatable, standard evaluation on modern, competitive tasks we use `init2winit` (Gilmer et al., 2021) for Jax (Bradbury et al., 2018) implementations of architectures in Flax (Heek et al., 2020) and standard dataset preprocessing built on top of TFDS (TFD, 2023). We rely on standard scientific packages for conducting our work (Waskom, 2021; Hunter, 2007; Harris et al., 2020; Virtanen et al., 2020). Our source code will be released after publication.

The main settings we explore are

- ResNet-50 (He et al., 2016) applied to the image classification task of ImageNet (Russakovsky et al., 2015) with cross entropy loss. Augmentations include only random cropping and flipping.
- A 16-layer Conformer model (Gulati et al., 2020) applied to the audio transcription dataset, LibriSpeech (Panayotov et al., 2015).
- A GNN with 5 message-passing steps (Battaglia et al., 2018) on `ogbg-molpcba` (Hu et al., 2020), which classifies structural properties of graphically encoded molecule inputs.

Our FD variant of Shampoo introduces only one new hyperparameter, the rank  $\ell$ , which we do not tune. We recommend setting it to be as large as memory allows in practice. We consider its effect in Sec. 5.3.

However, the baseline Shampoo, Adam, and the underlying architectures introduce their own hyperparameters, which we tune. FD-Shampoo inherits those of Shampoo.

### 5.1. Spectral Analysis

We inspect the exponential moving average of Kronecker-factored gradient covariance for fast spectral decay.

For all our architectures, we tune Shampoo and extract the intermediate gradient covariances over the course of training. To make our curves comparable across architectures, we fix the parameter for the second moment’s moving average,  $\beta_2 = 0.999$  for these runs. Furthermore, ResNet-50 has a

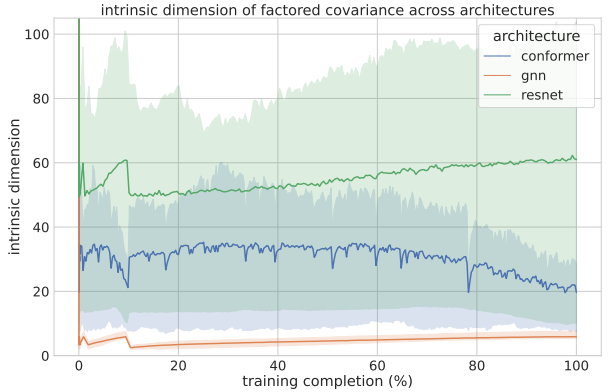


Figure 2: Intrinsic dimension  $\text{tr } C / \lambda_{\max}(C)$  of gradient covariance factors  $C$  across differing datasets and architectures. As in Fig. 1, we inspect covariance factors for each architecture for all dimensions of size 1024 (across all weights, the Conformer has 106 such dimensions, GNN has 10, and ResNet-50 has 79). We plot the average across all covariances for each network’s weight’s dimensions, with the shaded regions capturing the interquartile range.

few parameters with dimension 2048, but the largest dimension for any parameter from the other two architectures is 1024, so we use the Blocked Shampoo variant discussed in Sec. 2.4 with block size 1024. In other words, weights containing a dimension 2048 are split into two. We tune other Shampoo parameters for each architecture, and plot statistics of Kronecker factors  $L_t = \sum_i \beta_2^{t-i} G_t G_t^\top$  and  $R_t = \sum_i \beta_2^{t-i} G_t^\top G_t$ . Further details are available in Appendix B.

In Fig. 2, we plot the intrinsic dimension of Kronecker covariance factors over training for our three settings. The intrinsic dimension determines the rate at which empirical covariance estimates concentrate to their expectation, rather than a random vector’s actual dimension, up to logarithmic factors (Vershynin (2018), Remark 5.6.3). Despite actual dimensionality being over 1024, intrinsic dimension across all architectures stays below 105. A conspicuous phase shift 10% of the way through training may be the result of a change from linear learning rate warmup to a learning rate decay, starting at roughly 5% of the way into training.

Given  $\beta_2 = 0.999$ , we emphasize that the behavior in Fig. 2 is an emergent property of DL training. Though surely a lower  $\beta_2$  would naturally result in lower intrinsic dimension (which can still be taken advantage of by Alg. 2 and 3), we would still expect higher intrinsic dimension if covariances were near-isometries. If we observe some large number  $n = 10000$  draws  $x_i$  of  $1024 \times d$  matrices with iid  $N(0, 1)$  entries, then numerical experiments show that the average intrinsic dimension of  $\sum_{i=0}^{n-1} \beta_2^i x_i x_i^\top$  is 324.63

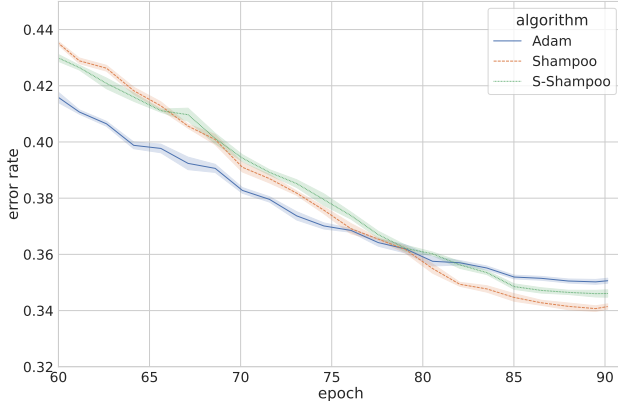


Figure 3: Test set performance on ImageNet v2 across 90 epochs of training on ImageNet v1, in terms of classification error rate for top-1 accuracy. We plot the mean of 5 random seeds, with 1.96 times the standard error as error bars. For readers familiar with ImageNet v1, final validation accuracy for Shampoo was 77.69% (0.03%), S-Shampoo having 77.18% (0.04%), and Adam having 76.76% (0.03%), but we emphasize that due to tuning, the test set performance pictured above should be of primary concern. This plot only shows the last 30 epochs of training, where the second order methods overtake Adam. Full curves are in Appendix C.

(0.52) and 862.13 (0.25) for  $d = 1, 64$ , respectively, with parenthesized numbers denoting standard error across 20 trials. Values generated this way are larger than the average intrinsic dimension of roughly 10, 30, 50 observed in Fig. 2.

## 5.2. Generalization Performance

To evaluate the effectiveness of S-Shampoo as a practical second-order algorithm for training networks, we perform a standard evaluation on the ResNet-50 architecture. We tune Adam, Shampoo, and S-Shampoo on ImageNet (Russakovsky et al., 2015), select hyperparameters based on validation set accuracy, and evaluate final test set performance using ImageNet v2 (Recht et al., 2019), as the ImageNet test set is unavailable. Hyperparameter tuning information is available in Appendix C; S-Shampoo inherits Shampoo’s hyperparameter space identically. The rank  $\ell$  for our FD sketches for each covariance factor is not tuned, we simply choose 256 based on our observations from Sec. 5.1.

As Fig. 3 demonstrates, the second-order information leveraged by Shampoo results in improvements over Adam, a first-order method. Our sketching approach falls in between the two, in line with the theoretical memory consumption of the three methods. With Librispeech, we find that performance does not match theoretical memory consumption; though Sketchy initially beats Adam, its generalization performance is eventually surpassed by the first-order method

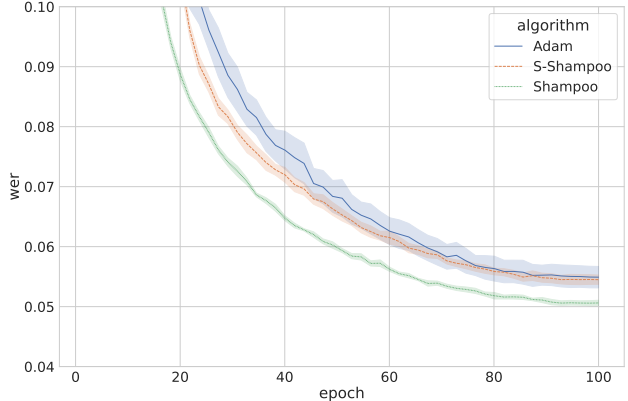


Figure 4: Test set performance on Librispeech across 100 epochs of training, in terms of word error rate (WER). Training details are available in Appendix D. The mean of 5 random seeds is plotted, with 1.96 times the standard error as error bars. Despite stronger initial performance, Sketchy ends up slightly better but still close to Adam in terms of final WER. As discussed in Sec. 5.2, not all problems are amenable to second-order methods and we anticipate that Sketchy will improve over first-order methods in those where the distinction is large. The second-order methods have much smaller spread than Adam.

(Fig. 4). In this example, the generalization benefits from the second order method, Shampoo, are not much larger than that of the first order method. As a result, the quality degradation from constrained memory use results in worsened performance in the end. Despite this, for problems where second order information results in generalization advantages, Sketchy may be an attractive option.

## 5.3. Training Improvement

In contrast to Sec. 5.2, to assess training optimization quality, we must fix regularization constants to make training curves comparable, whereas standard practice mandates tuning regularization (such as weight decay and dropout rate). Details are available in Appendix E. As Fig. 5 demonstrates, increases in rank improve optimization.

## 6. Discussion

Up to spectral error, Alg. 2 achieves full-matrix AdaGrad regret despite approximating the *smallest* part of the spectrum of  $G_t^{-1/2}$  at each step. Remarkably, these eigenvectors correspond to the *most* easily discernible signals of the covariance for the stream  $g_t$ . This apparent (and fortuitous) coincidence is resolved by considering the covariance of  $\tilde{G}_t^{-1/2} g_t$ : whitening the gradient to facilitate optimization best reflects on regret; as a result, approximating top eigenvectors of  $G_T$  helps more than the bottom ones.

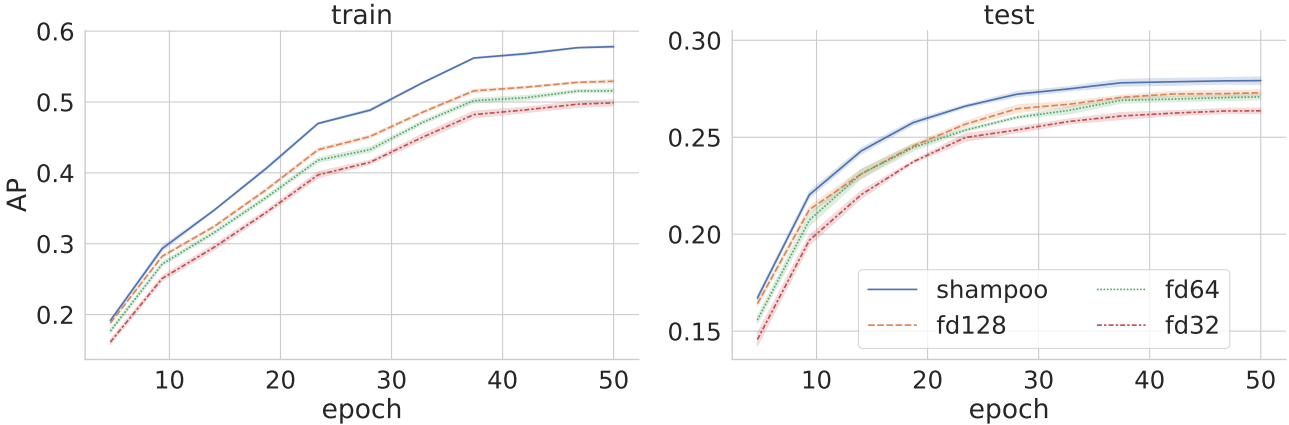


Figure 5: ogbg-molpcba train and test set performance with the GNN model across 50 epochs of training, in terms of average precision (AP, higher is better), based on validation-tuned parameters, with the mean of 5 random seeds plotted and standard errors shaded. Training curves reflect growing rank improving training AP, with Shampoo at the upper limit of training performance (fdN refers to S-Shampoo with rank N). Though generalization behavior may have less obvious gradation, it largely follows the same trend of low rank S-Shampoo, larger-rank S-Shampoo, and finally Shampoo.

Our initial implementation focused on correctness rather than physical speed or memory reduction. Engineering optimizers competitive with existing industrial-strength implementations of Adam and Shampoo was out of scope. In implementing FD, we performed updates via the factored SVD of  $[\beta_2^{1/2} B_t; G_t]$  rather than the eigendecomposition depicted in Alg. 1; this avoids squaring, which is unavoidable in Shampoo. For speed, Shampoo subsamples gradients for its covariance estimation and updates its inverse matrix roots intermittently, every fixed number of steps. A tuning script provided by Anil et al. (2020) included gradients from every step, but updated roots every 10 steps. Since FD does not separate sampling from its computation of estimated covariance eigendecomposition, we took the more difficult setting for S-Shampoo, only allowing it to simultaneously observe every 10<sup>th</sup> gradient and update its covariance inverse roots (see Appendix F for a theoretical justification).

Though step-skipping makes Shampoo and S-Shampoo tractable, future work may explore further speedups: since FD only requires the top  $\ell$  eigenvalues, iterative Lanczos-like routines which are accelerator-friendly, such as LOBPCG (Knyazev, 2001), may allow incremental updates to  $\tilde{G}_t^{-1/2}$  in factored form with only a few matrix multiplies, S-Shampoo may be able to update more frequently than its non-sketched counterpart, further improving quality.

## 7. Conclusion

In this work, we address a gap in the OCO literature for low-memory optimization with the novel Alg. 2 and demonstrate its relevance to practical non-convex problems such as neural net training (Sec. 5.2) by leveraging a new observation

about gradient covariance (Sec. 5.1).

The growing disparity between compute capability and memory bandwidth (Jouppi et al., 2021) underscores the need for further research in this direction. Further, in large-batch settings, the disparity between first and second order methods demands approximations which close the performance gap between the two. Even in performing experiments for this work, we would frequently find that faster accelerators were unavailable, but many previous-generation ones were, encouraging us to leverage data-parallel training. For datasets such as Imagenet, we notice the advantage of second order methods in dealing with large batches even at relatively modest sizes, such as 1024; many works on explore several larger multiples of this (Keskar et al., 2016).

Potential for future work includes numerical methods outlined in the previous section as well optimizing the rank  $\ell$  across the many tensors in a network, as the spread in Fig. 2 highlights the large variance in covariance intrinsic dimension. Furthermore, the inductive biases conferred by the minima which different-rank representations of curvature reach may have problem-dependent generalization implications, a question which we leave for future work. For a comparison of full rank preconditioning’s effect versus first-order minima, see Amari et al. (2020).

**Broader impacts.** As a method which reduces memory consumption for second-order methods, our work will make use cases which rely on such curvature have a lower barrier to entry. A negative effect may be increased electricity consumption from new trainings resulting from this availability.

## References

Tensorflow datasets, a collection of ready-to-use datasets. <https://www.tensorflow.org/datasets>, 2023.

Agarwal, N., Allen-Zhu, Z., Bullins, B., Hazan, E., and Ma, T. Finding approximate local minima faster than gradient descent. In *Proceedings of the 49th Annual ACM SIGACT Symposium on Theory of Computing*, pp. 1195–1199, 2017.

Agarwal, N., Bullins, B., Chen, X., Hazan, E., Singh, K., Zhang, C., and Zhang, Y. Efficient full-matrix adaptive regularization. In Chaudhuri, K. and Salakhutdinov, R. (eds.), *Proceedings of the 36th International Conference on Machine Learning*, volume 97 of *Proceedings of Machine Learning Research*, pp. 102–110. PMLR, 09–15 Jun 2019.

Agarwal, N., Anil, R., Hazan, E., Koren, T., and Zhang, C. Disentangling adaptive gradient methods from learning rates. *arXiv preprint arXiv:2002.11803*, 2020.

Amari, S.-i., Ba, J., Grosse, R. B., Li, X., Nitanda, A., Suzuki, T., Wu, D., and Xu, J. When does preconditioning help or hurt generalization? In *International Conference on Learning Representations*, 2020.

Ando, T. Concavity of certain maps on positive definite matrices and applications to hadamard products. *Linear algebra and its applications*, 26:203–241, 1979.

Anil, R., Gupta, V., Koren, T., and Singer, Y. Memory efficient adaptive optimization. *Advances in Neural Information Processing Systems*, 32, 2019.

Anil, R., Gupta, V., Koren, T., Regan, K., and Singer, Y. Scalable second order optimization for deep learning. *arXiv preprint arXiv:2002.09018*, 2020.

Audenaert, K. M. A generalisation of mirsky’s singular value inequalities. *arXiv preprint arXiv:1410.4941*, 2014.

Ba, J. L., Kiros, J. R., and Hinton, G. E. Layer normalization. *arXiv preprint arXiv:1607.06450*, 2016.

Bakker, C., Henry, M. J., and Hodas, N. O. Understanding and exploiting the low-rank structure of deep networks. 2018.

Battaglia, P. W., Hamrick, J. B., Bapst, V., Sanchez-Gonzalez, A., Zambaldi, V., Malinowski, M., Tacchetti, A., Raposo, D., Santoro, A., Faulkner, R., et al. Relational inductive biases, deep learning, and graph networks. *arXiv preprint arXiv:1806.01261*, 2018.

Bhatia, R. *Matrix analysis*. Springer, 1997.

Bradbury, J., Frostig, R., Hawkins, P., Johnson, M. J., Leary, C., Maclaurin, D., Necula, G., Paszke, A., VanderPlas, J., Wanderman-Milne, S., and Zhang, Q. JAX: composable transformations of Python+NumPy programs, 2018.

Brockett, R. W. *Finite dimensional linear systems*. SIAM, 2015.

Bubeck, S. et al. Convex optimization: Algorithms and complexity. *Foundations and Trends® in Machine Learning*, 8(3-4):231–357, 2015.

Chen, X., Agarwal, N., Hazan, E., Zhang, C., and Zhang, Y. Extreme tensoring for low-memory preconditioning. In *International Conference on Learning Representations*, 2019.

Cutkosky, A. Better full-matrix regret via parameter-free online learning. In Larochelle, H., Ranzato, M., Hadsell, R., Balcan, M., and Lin, H. (eds.), *Advances in Neural Information Processing Systems*, volume 33, pp. 8836–8846. Curran Associates, Inc., 2020.

Dally, W. J., Keckler, S. W., and Kirk, D. B. Evolution of the graphics processing unit (gpu). *IEEE Micro*, 41(6): 42–51, 2021.

Dayma, B. and Anil, R. Evaluation of Distributed Shampoo: Comparison of optimizers: Distributed Shampoo, Adam & Adafactor. *Weights & Biases Report*, 2022.

Devlin, J., Chang, M.-W., Lee, K., and Toutanova, K. Bert: Pre-training of deep bidirectional transformers for language understanding. In *Proceedings of the 2019 Conference of the North American Chapter of the Association for Computational Linguistics: Human Language Technologies, Volume 1 (Long and Short Papers)*, pp. 4171–4186, 2019.

Duchi, J., Hazan, E., and Singer, Y. Adaptive subgradient methods for online learning and stochastic optimization. *Journal of machine learning research*, 12(7), 2011.

Ghashami, M., Liberty, E., Phillips, J. M., and Woodruff, D. P. Frequent directions: Simple and deterministic matrix sketching. *SIAM Journal on Computing*, 45(5):1762–1792, 2016.

Ghorbani, B., Krishnan, S., and Xiao, Y. An investigation into neural net optimization via hessian eigenvalue density. In *International Conference on Machine Learning*, pp. 2232–2241. PMLR, 2019.

Gilmer, J. M., Dahl, G. E., and Nado, Z. init2winit: a jax codebase for initialization, optimization, and tuning research, 2021. URL <http://github.com/google/init2winit>.

Gulati, A., Qin, J., Chiu, C.-C., Parmar, N., Zhang, Y., Yu, J., Han, W., Wang, S., Zhang, Z., Wu, Y., et al. Conformer: Convolution-augmented transformer for speech recognition. *arXiv preprint arXiv:2005.08100*, 2020.

Gupta, V., Koren, T., and Singer, Y. Shampoo: Preconditioned stochastic tensor optimization. In *International Conference on Machine Learning*, pp. 1842–1850. PMLR, 2018.

Gur-Ari, G., Roberts, D. A., and Dyer, E. Gradient descent happens in a tiny subspace. *arXiv preprint arXiv:1812.04754*, 2018.

Harris, C. R., Millman, K. J., van der Walt, S. J., Gommers, R., Virtanen, P., Cournapeau, D., Wieser, E., Taylor, J., Berg, S., Smith, N. J., Kern, R., Picus, M., Hoyer, S., van Kerkwijk, M. H., Brett, M., Haldane, A., del Rio, J. F., Wiebe, M., Peterson, P., Gérard-Marchant, P., Sheppard, K., Reddy, T., Weckesser, W., Abbasi, H., Gohlke, C., and Oliphant, T. E. Array programming with NumPy. *Nature*, 585(7825):357–362, September 2020. doi: 10.1038/s41586-020-2649-2.

Hazan, E. Lecture notes: Optimization for machine learning. *arXiv preprint arXiv:1909.03550*, 2019.

Hazan, E. et al. Introduction to online convex optimization. *Foundations and Trends® in Optimization*, 2(3-4):157–325, 2016.

He, K., Zhang, X., Ren, S., and Sun, J. Deep residual learning for image recognition. In *Proceedings of the IEEE conference on computer vision and pattern recognition*, pp. 770–778, 2016.

Heek, J., Levskaya, A., Oliver, A., Ritter, M., Rondepierre, B., Steiner, A., and van Zee, M. Flax: A neural network library and ecosystem for JAX, 2020.

Hinton, G., Srivastava, N., and Swersky, K. Neural networks for machine learning lecture 6a overview of mini-batch gradient descent. *Cited on*, 14(8):2, 2012.

Hu, W., Fey, M., Zitnik, M., Dong, Y., Ren, H., Liu, B., Catasta, M., and Leskovec, J. Open graph benchmark: Datasets for machine learning on graphs. In Larochelle, H., Ranzato, M. A., Hadsell, R., Balcan, M., and Lin, H. (eds.), *Advances in Neural Information Processing Systems 33: Annual Conference on Neural Information Processing Systems 2020, NeurIPS 2020, December 6-12, 2020, virtual*, 2020.

Hunter, J. D. Matplotlib: A 2d graphics environment. *Computing in Science & Engineering*, 9(3):90–95, 2007. doi: 10.1109/MCSE.2007.55.

Jouppi, N. P., Yoon, D. H., Ashcraft, M., Gottscho, M., Jablin, T. B., Kurian, G., Laudon, J., Li, S., Ma, P., Ma, X., et al. Ten lessons from three generations shaped google’s tpuv4i: Industrial product. In *2021 ACM/IEEE 48th Annual International Symposium on Computer Architecture (ISCA)*, pp. 1–14. IEEE, 2021.

Kalai, A. and Vempala, S. Efficient algorithms for online decision problems. *Journal of Computer and System Sciences*, 71(3):291–307, 2005.

Keskar, N. S., Mudigere, D., Nocedal, J., Smelyanskiy, M., and Tang, P. T. P. On large-batch training for deep learning: Generalization gap and sharp minima. *arXiv preprint arXiv:1609.04836*, 2016.

Kingma, D. P. and Ba, J. Adam: A method for stochastic optimization. In *ICLR (Poster)*, 2015.

Knyazev, A. V. Toward the optimal preconditioned eigensolver: Locally optimal block preconditioned conjugate gradient method. *SIAM journal on scientific computing*, 23(2):517–541, 2001.

Krummenacher, G., McWilliams, B., Kilcher, Y., Buhmann, J. M., and Meinshausen, N. Scalable adaptive stochastic optimization using random projections. *Advances in Neural Information Processing Systems*, 29, 2016.

Liberty, E. Even simpler deterministic matrix sketching. *arXiv preprint arXiv:2202.01780*, 2022.

Luo, H., Agarwal, A., Cesa-Bianchi, N., and Langford, J. Efficient second order online learning by sketching. *Advances in Neural Information Processing Systems*, 29, 2016.

Martens, J. and Grosse, R. Optimizing neural networks with kronecker-factored approximate curvature. In *International conference on machine learning*, pp. 2408–2417. PMLR, 2015.

MLCommons® open engineering consortium. MLCommons Algorithmic Efficiency. <https://github.com/mlcommons/algorithmic-efficiency>, 2023.

Panayotov, V., Chen, G., Povey, D., and Khudanpur, S. LibriSpeech: an asr corpus based on public domain audio books. In *Acoustics, Speech and Signal Processing (ICASSP), 2015 IEEE International Conference on*, pp. 5206–5210. IEEE, 2015.

Petersen, K. B., Pedersen, M. S., et al. The matrix cookbook. *Technical University of Denmark*, 7(15):510, 2008.

Recht, B., Roelofs, R., Schmidt, L., and Shankar, V. Do imagenet classifiers generalize to imagenet? In *International Conference on Machine Learning*, pp. 5389–5400, 2019.

Reddi, V. J., Cheng, C., Kanter, D., Mattson, P., Schmuelling, G., Wu, C.-J., Anderson, B., Breughe, M., Charlebois, M., Chou, W., Chukka, R., Coleman, C., Davis, S., Deng, P., Diamos, G., Duke, J., Fick, D., Gardner, J. S., Hubara, I., Idgunji, S., Jablin, T. B., Jiao, J., John, T. S., Kanwar, P., Lee, D., Liao, J., Lokhmotov, A., Massa, F., Meng, P., Micikevicius, P., Osborne, C., Pekhimenko, G., Rajan, A. T. R., Sequeira, D., Sirasao, A., Sun, F., Tang, H., Thomson, M., Wei, F., Wu, E., Xu, L., Yamada, K., Yu, B., Yuan, G., Zhong, A., Zhang, P., and Zhou, Y. Mlperf inference benchmark, 2019.

Russakovsky, O., Deng, J., Su, H., Krause, J., Satheesh, S., Ma, S., Huang, Z., Karpathy, A., Khosla, A., Bernstein, M., Berg, A. C., and Fei-Fei, L. ImageNet Large Scale Visual Recognition Challenge. *International Journal of Computer Vision (IJCV)*, 115(3):211–252, 2015. doi: 10.1007/s11263-015-0816-y.

Sagun, L., Bottou, L., and LeCun, Y. Eigenvalues of the hessian in deep learning: Singularity and beyond. *arXiv preprint arXiv:1611.07476*, 2016.

Sagun, L., Evci, U., Guney, V. U., Dauphin, Y., and Bottou, L. Empirical analysis of the hessian of over-parametrized neural networks. *arXiv preprint arXiv:1706.04454*, 2017.

Sankar, A. R., Khasbage, Y., Vigneswaran, R., and Balasubramanian, V. N. A deeper look at the hessian eigen-spectrum of deep neural networks and its applications to regularization. In *Proceedings of the AAAI Conference on Artificial Intelligence*, volume 35, pp. 9481–9488, 2021.

Shazeer, N. and Stern, M. Adafactor: Adaptive learning rates with sublinear memory cost. In *International Conference on Machine Learning*, pp. 4596–4604. PMLR, 2018.

Shazeer, N., Mirhoseini, A., Maziarz, K., Davis, A., Le, Q., Hinton, G., and Dean, J. Outrageously large neural networks: The sparsely-gated mixture-of-experts layer. *arXiv preprint arXiv:1701.06538*, 2017.

Vershynin, R. *High-dimensional probability: An introduction with applications in data science*, volume 47. Cambridge university press, 2018.

Virtanen, P., Gommers, R., Oliphant, T. E., Haberland, M., Reddy, T., Cournapeau, D., Burovski, E., Peterson, P., Weckesser, W., Bright, J., van der Walt, S. J., Brett, M., Wilson, J., Millman, K. J., Mayorov, N., Nelson, A. R. J., Jones, E., Kern, R., Larson, E., Carey, C. J., Polat, İ., Feng, Y., Moore, E. W., VanderPlas, J., Laxalde, D., Perktold, J., Cimrman, R., Henriksen, I., Quintero, E. A., Harris, C. R., Archibald, A. M., Ribeiro, A. H., Pedregosa, F., van Mulbregt, P., and SciPy 1.0 Contributors. SciPy 1.0: Fundamental Algorithms for Scientific Computing in Python. *Nature Methods*, 17:261–272, 2020. doi: 10.1038/s41592-019-0686-2.

Wan, Y. and Zhang, L. Efficient adaptive online learning via frequent directions. *IEEE Transactions on Pattern Analysis and Machine Intelligence*, 2021.

Waskom, M. L. seaborn: statistical data visualization. *Journal of Open Source Software*, 6(60):3021, 2021. doi: 10.21105/joss.03021.

Xie, Z., Tang, Q.-Y., He, Z., Sun, M., and Li, P. Rethinking the structure of stochastic gradients: Empirical and statistical evidence. *arXiv preprint arXiv:2212.02083*, 2022.

## A. Proof details

**Notation.** Let  $\|\cdot\|$  denote the  $\ell_2$  norm for a vector. Let  $\|\cdot\|_{op}$ ,  $\|\cdot\|_F$  denote the operator norm and the Frobenius norm of a matrix, respectively. For a positive definite matrix  $A$ , we use  $\|x\|_A = \sqrt{x^\top A x}$  to denote the matrix norm induced by  $A$ , and  $\|x\|_A^* = \sqrt{x^\top A^{-1} x}$  to denote the dual norm of the induced matrix norm. For a matrix  $A$ ,  $A^{-1}$  is the inverse of  $A$  if  $A$  is full rank; otherwise,  $A^{-1}$  is taken to be the Moore-Penrose pseudoinverse. Finally,  $\bar{\text{vec}}(\cdot)$  denotes the row-major vectorization of a given matrix, and  $\otimes$  denotes the Kronecker product between two matrices

### A.1. Proof of Observation 1

*Proof.* Let  $\Sigma = \mathbb{E}[g_t g_t^\top]$  denote the covariance of the gradients, and  $\lambda_i = \lambda_i(\Sigma)$  denote its  $i$ -th eigenvalue. By definition,  $g_t$  has the following distribution:  $g_t = w_i$  with probability  $\lambda_i$ . At iteration  $t$ , we have the current sketch  $\bar{G}_{t-1} \in \mathbb{R}^{\ell \times d}$ , and we receive the new gradient  $g_t$ . Ada-FD uses  $\bar{G}_{t-1} + \delta I$  as their preconditioner.

We first show that under the distribution of the cost functions, if  $\bar{G}_{t-1}$  has rank  $\ell - 1$ , then  $\mathbb{E}[\rho_t | \bar{G}_{t-1}] \geq \sum_{i=\ell}^r \lambda_i$ . Let  $\bar{G}_{t-1} = U \Sigma V^\top$  be the SVD of  $\bar{G}_{t-1}$ , and  $v_i$  be the  $i$ -th row of  $V \in \mathbb{R}^{\ell-1 \times d}$ . Let  $N_{t-1} = W \setminus \{v_1, \dots, v_{\ell-1}\}$  be the set of basis vectors not in the row space of  $\bar{G}_{t-1}$ , then  $|N_{t-1}| = r - \ell + 1$ . If  $g_t \in \text{span}(v_1, \dots, v_\ell)$ , then  $\rho_t = 0$ ; otherwise  $\rho_t = 1$ , with probability  $\sum_{i:w_i \in N_{t-1}} \lambda_i \geq \sum_{i=\ell}^r \lambda_i$ .

We proceed to bound the probability that  $\bar{G}_{t-1}$  has rank  $\ell' \leq \ell - 2$ . Note that this event is equivalent to having fewer than  $\ell - 1$  distinct vectors drawn from  $W$ . Let  $I_i$  be the indicator variable for drawing  $w_i$  in the first  $t - 1$  rounds, then we can obtain the expected number of distinct vectors as follows

$$\mathbb{E} \left[ \sum_{i=1}^r I_i \right] = \sum_{i=1}^r \mathbb{E}[I_i] = \sum_{i=1}^r 1 - (1 - \lambda_i)^{t-1}.$$

We consider the random variable  $r - \sum_{i=1}^r I_i$ , and by Markov's inequality,

$$\begin{aligned} \mathbb{P} \left[ r - \sum_{i=1}^r I_i \geq r - \ell + 2 \right] &\leq \frac{\sum_{i=1}^r (1 - \lambda_i)^{t-1}}{r - \ell + 2} \\ &\leq \frac{r(1 - \lambda_r)^{t-1}}{2}. \end{aligned}$$

Note that this is exactly the probability of having fewer than  $\ell - 1$  distinct vectors in the first  $t - 1$  draws. We conclude that for  $t \geq \log r / \lambda_r + 1$ ,  $\mathbb{P}[\text{rank}(\bar{G}_{t-1}) = \ell - 1] \geq \frac{1}{2}$ . This implies that  $\mathbb{E}[\rho_t] \geq \sum_{i=\ell}^r \lambda_i / 2$  after an initial log

number of rounds, and assuming  $T \geq 2 \log r / \lambda_r$ ,

$$\mathbb{E} \left[ \sum_{t=1}^T \rho_t \right] \geq \mathbb{E} \left[ \sum_{t=T/2+1}^T \rho_t \right] \geq \frac{T}{4} \sum_{i=\ell}^r \lambda_i.$$

Similarly,

$$\mathbb{E} \left[ \sum_{t=1}^T \sqrt{\rho_t} \right] \geq \mathbb{E} \left[ \sum_{t=T/2+1}^T \sqrt{\rho_t} \right] \geq \frac{T}{4} \sum_{i=\ell}^r \lambda_i,$$

where the second inequality holds because  $\rho_t = 0$  or  $1$ , so  $\sqrt{\rho_t} = \rho_t$  for all  $t$ . The quantities  $\sum_{t=1}^T \rho_t$  and  $\sum_{t=1}^T \sqrt{\rho_t}$  correspond to  $\Delta_T$  and  $\sum_{t=1}^T \sqrt{\sigma_t}$  in Theorem 1 of (Wan & Zhang, 2021), respectively. Therefore, under our setting, the expectation of the upper bound in Theorem 1 is at least

$$\begin{aligned} &\eta \mathbb{E} \left[ \max \left\{ 1, \frac{1 + \sqrt{\sum_{t=1}^T \rho_t}}{\delta} \right\} \text{tr}(G_T^{1/2}) \right] \\ &+ \frac{D^2}{2\eta} \mathbb{E} \left[ \sum_{t=1}^T \sqrt{\rho_t} \right]. \end{aligned} \tag{1}$$

If we can tune  $\delta$ , then the max function evaluates to at least 1, and

$$\begin{aligned} (1) &\geq \eta \mathbb{E} \left[ \text{tr}(G_T^{1/2}) \right] + \frac{D^2}{2\eta} \frac{T}{4} \sum_{i=\ell}^r \lambda_i \\ &\geq \eta \mathbb{E} \left[ \sqrt{\text{tr}(G_T)} \right] + \frac{D^2 T}{8\eta} \sum_{i=\ell}^r \lambda_i \\ &= \eta \sqrt{T} + \frac{D^2 T}{8\eta} \sum_{i=\ell}^r \lambda_i, \end{aligned}$$

where the last equality holds because  $\text{tr}(G_T) = \sum_{t=1}^T \|g_t\|_2^2 = T$ . Optimizing  $\eta$ , we conclude that the regret upper bound for Ada-FD is  $\Omega(T^{3/4})$  in expectation.  $\square$

### A.2. Proof details for Section 4.1, S-AdaGrad

#### A.2.1. PROOF OF THEOREM 3

The following observations are made of Algorithm 1:

**Observation 7.** Denote by  $\bar{U}_t \stackrel{\text{def}}{=} [U_t; U_t^\perp]$ . If each  $M_t$  is of rank 1, then

$$\bar{G}_t + \lambda_\ell^{(t)} I = \bar{G}_{t-1} + M_t + \lambda_\ell^{(t)} N_t,$$

where  $N_t = U_t^\perp (U_t^\perp)^\top$ .

*Proof.* By definition of Algorithm 1,  $\bar{G}_{t-1} = B_{t-1}B_{t-1}^\top$  is of rank at most  $\ell - 1$ . Under the assumption that  $M_t$  is of rank 1,  $\bar{G}_{t-1} + M_t$  is of rank at most  $\ell$ . Therefore,  $\lambda_{\ell+1:d} = 0$ . Then, we have the following:

$$\begin{aligned}\bar{G}_t + \lambda_\ell^{(t)} I &= U_t \operatorname{diag} \left( \lambda_{[1:\ell]}^{(t)} - \lambda_\ell^{(t)} \right) U_t^\top + \lambda_\ell^{(t)} I \\ &= U_t \operatorname{diag} \left( \lambda_{[1:\ell]}^{(t)} - \lambda_\ell^{(t)} \right) U_t^\top + \lambda_\ell^{(t)} (U_t U_t^\top + N_t) \\ &= U_t \operatorname{diag} \lambda_{[1:\ell]}^{(t)} U_t^\top + \lambda_\ell^{(t)} N_t \\ &= \bar{U}_t \operatorname{diag} \lambda^{(t)} \bar{U}_t^\top + \lambda_\ell^{(t)} N_t \\ &= \bar{G}_{t-1} + M_t + \lambda_\ell^{(t)} N_t.\end{aligned}$$

□

**Lemma 8.** Let  $\lambda_\ell^{(s:t)}$  denote  $\sum_{j=s}^t \lambda_\ell^{(j)}$ . Let  $\tilde{G}_t \stackrel{\text{def}}{=} \bar{G}_t + \lambda_\ell^{(1:t)} I$ ,  $G_t = \sum_{s=1}^t M_s$ , where each  $M_t$  is of rank 1. Let the initial  $G_0 = \tilde{G}_0 = 0$ , then the following relation between  $\tilde{G}_t$  and  $G_t$  holds for all  $t$ :

$$\tilde{G}_t = G_t + \sum_{s=1}^t \lambda_\ell^{(s)} N_s.$$

*Proof.* The lemma follows from induction on  $t$ . Base case  $\tilde{G}_0 = G_0$  holds by definition. Suppose the above equation holds for  $t - 1$ . Then,

$$\begin{aligned}\tilde{G}_t &= \bar{G}_t + \lambda_\ell^{(1:t)} I =_1 \bar{G}_{t-1} + M_t + \lambda_\ell^{(t)} N_t + \lambda_\ell^{(1:t-1)} I \\ &= \tilde{G}_{t-1} + M_t + \lambda_\ell^{(t)} N_t \\ &=_2 G_{t-1} + \sum_{s=1}^{t-1} \lambda_\ell^{(s)} N_s + M_t + \lambda_\ell^{(t)} N_t \\ &= G_t + \sum_{s=1}^t \lambda_\ell^{(s)} N_s,\end{aligned}$$

where  $=_1$  follows from Observation 7 and  $=_2$  follows from induction hypothesis. □

**Remark 9.** Note that the above lemma immediately provides an approximate isometry  $\tilde{G}_t \preceq G_t \preceq \tilde{G}_t$ .

Now, we return to the proof of Thm. 3.

*Proof.* First, we make the following observation of Algorithm 2:

**Observation 10.** By specification of Algorithm 1,2,  $g_t \in \operatorname{span}(\tilde{G}_t)$ ,  $\forall t$ .

We follow the standard AdaGrad (Duchi et al., 2011; Hazan et al., 2016) analysis. By algorithm specification,

$$\begin{aligned}y_{t+1} - x^* &= x_t - x^* - \eta \tilde{G}_t^{-1/2} g_t, \\ \tilde{G}_t^{1/2} (y_{t+1} - x^*) &= \tilde{G}_t^{1/2} (x_t - x^*) - \eta \tilde{G}_t^{1/2} \tilde{G}_t^{-1/2} g_t \\ &=_1 \tilde{G}_t^{1/2} (x_t - x^*) - \eta g_t,\end{aligned}$$

where  $=_1$  follows from Observation 10.

With standard AdaGrad analysis, we can bound regret  $\operatorname{Regret}_T$  above by the sum of the diameter bound and the gradient bound:

$$\underbrace{\frac{1}{2\eta} \sum_{t=1}^T \|x_t - x^*\|_{\tilde{G}_t^{1/2} - \tilde{G}_{t-1}^{1/2}}^2}_{R_D} + \underbrace{\frac{\eta}{2} \sum_{t=1}^T \|g_t\|_{F_t^{-1/2}}}_{R_G}.$$

Note that by algorithm specification, we have  $\forall t$ ,

$$\tilde{G}_t = \bar{G}_t + \rho_{1:t} I =_1 \tilde{G}_{t-1} + g_t g_t^\top + \rho_t N_t \succeq \tilde{G}_{t-1} + g_t g_t^\top,$$

where  $=_1$  follows from the proof of Lemma 8. In particular,  $\tilde{G}_t \succeq \tilde{G}_{t-1}$ .

Using Remark 9, the gradient norm term in the regret bound can be further bounded by

$$\begin{aligned}R_G &= \frac{\eta}{2} \sum_{t=1}^T g_t^\top \tilde{G}_t^{-1/2} g_t \\ &\leq \frac{\eta}{2} \sum_{t=1}^T g_t^\top G_t^{-1/2} g_t \leq \eta \operatorname{tr} \left( G_T^{1/2} \right),\end{aligned}$$

where the last inequality follows from Lemma 10 of Duchi et al. (2011).<sup>2</sup> The diameter norm term in the regret bound can be bounded by

$$\begin{aligned}R_D &= \frac{1}{2\eta} \sum_{t=1}^T \|x_t - x^*\|_{\tilde{G}_t^{1/2} - \tilde{G}_{t-1}^{1/2}}^2 \leq_1 \frac{D^2}{2\eta} \operatorname{tr} \left( \tilde{G}_T^{1/2} \right) \\ &\leq \frac{D^2}{2\eta} \operatorname{tr} \left( (G_T + \rho_{1:T} I)^{1/2} \right) \\ &\leq_2 \frac{D^2}{2\eta} \left( \operatorname{tr} G_T^{1/2} + \operatorname{tr} (\rho_{1:T} I)^{1/2} \right),\end{aligned}$$

where  $\leq_1$  follows from monotonicity of  $\tilde{G}_t$ 's,  $\|\cdot\|_{op} \leq \operatorname{tr}(\cdot)$  for positive semidefinite matrices, and linearity of  $\operatorname{tr}(\cdot)$ , and  $\leq_2$  follows from that for  $X \in \mathbb{R}^d$ ,  $X \succeq 0$ ,  $\operatorname{tr}(X + \sigma I_d)^{1/2} \leq \operatorname{tr}(X^{1/2}) + d\sqrt{\sigma}$ . Combining, we have

$$\begin{aligned}\operatorname{Regret}_T &\leq \frac{d\sqrt{\rho_{1:T}} + \operatorname{tr} G_T^{1/2}}{2\eta} D^2 + \eta \operatorname{tr} \left( G_T^{1/2} \right) \\ &= D \left( \sqrt{2} \operatorname{tr} G_T^{1/2} + d\sqrt{\frac{\rho_{1:T}}{2}} \right),\end{aligned}$$

where the last equality is established by choosing  $\eta = \frac{D}{\sqrt{2}}$ . □

<sup>2</sup>The FTL-BTL lemma (Kalai & Vempala, 2005) alone is not sufficient to justify this inequality, at least interpreting  $G^{-1/2}$  as  $(G^{1/2})^+$ . However, Duchi et al. (2011) rely on concavity of  $X \mapsto \operatorname{tr} X^{1/2}$  to show a semidefinite version of the statement.

### A.2.2. PROOF OF COROLLARY 4

*Proof.* Following the proof of Theorem 3, we have

$$\text{Regret}_T \leq \frac{D^2 \text{tr } \tilde{G}_T^{1/2}}{2\eta} + \eta \text{tr } G_T^{1/2},$$

Denote the accumulated error term

$$E = \sum_{t=1}^T \rho_t N_t.$$

Then, by Lemma 8 and sub-additivity of  $\text{tr}((\cdot)^{1/2})$  (Audebert, 2014),

$$\text{Regret}_T \leq \left( \frac{D^2}{2\eta} + \eta \right) \text{tr } G_T^{1/2} + \frac{D^2}{2\eta} \text{tr } E^{1/2},$$

where it remains to bound the last term. Let  $Q$  be a matrix with column vectors  $q_i$  that forms an eigenbasis of  $E^{1/2}$ ; this diagonalizes  $E$  as well. Notice that

$$\lambda_i(E) = \sum_{t=1}^T \rho_t q_i^\top N_t q_i,$$

and since

$$\lambda_i^{1/2}(E) = \lambda_i(E^{1/2}),$$

that we can characterize

$$\text{tr } E^{1/2} = \sum_{i=1}^d \lambda_i^{1/2}(E) = \sum_{i=1}^d \left( \sum_{t=1}^T \rho_t q_i^\top N_t q_i \right)^{1/2}.$$

Denote  $u_{t,i} = q_i^\top N_t q_i$ , since  $N_t$  is a rank- $(d-\ell)$  projection,  $\|u_t\|_1 = d-\ell$ . Then  $\text{tr } E^{1/2}$  is upper bounded by the value of the program

$$\begin{aligned} \max_{u_{t,i}} \quad & \sum_{i=1}^d \left( \sum_{t=1}^T \rho_t u_{t,i} \right)^{1/2} \\ \text{s.t.} \quad & \sum_{i=1}^d u_{t,i} = d-\ell \quad \forall t \in [T]. \end{aligned}$$

Note that

$$\begin{aligned} \sum_{i=1}^d \left( \sum_{t=1}^T \rho_t u_{t,i} \right)^{1/2} & \leq_1 \sqrt{d} \sqrt{\sum_{i=1}^d \sum_{t=1}^T \rho_t u_{t,i}} \\ & = \sqrt{d} \sqrt{\sum_{t=1}^T \rho_t \sum_{i=1}^d u_{t,i}} \\ & =_2 \sqrt{d \rho_{1:T} (d-\ell)}, \end{aligned}$$

where  $\leq_1$  follows from Cauchy-Schwarz, and  $=_2$  follows from the constraint on  $\sum_{i=1}^d u_{t,i}$ .

Combining, we have

$$\begin{aligned} \text{Regret}_T & \leq \frac{\sqrt{d(d-\ell) \rho_{1:T}} + \text{tr } G_T^{1/2}}{2\eta} D^2 + \eta \text{tr } G_T^{1/2} \\ & = D \left( \sqrt{2} \text{tr } G_T^{1/2} + \sqrt{\frac{d(d-\ell) \rho_{1:T}}{2}} \right), \end{aligned}$$

where the last equality follows from the choice of step size  $\eta = \frac{D}{\sqrt{2}}$ .  $\square$

### A.2.3. PROOF OF LEM. 2

*Proof.* Let  $H_T \in \mathbb{R}^{T \times d}$  denote the matrix of stacked gradients, where the  $t$ -th row of  $H_T$  is  $g_t$ . Then  $H_T^\top H_T = G_T$ , and FD iteratively sketches  $H_T$ . Let  $H_T = U \Sigma V^\top$  be the SVD of  $H_T$ , and let  $H_{T,k} = U_k \Sigma_k V_k^\top$  denote the best rank- $k$  approximation of  $H_T$ , where  $U_k, V_k$  are the first  $k$  columns of the matrices, and  $\Sigma_k$  is the upper left  $k \times k$  submatrix of  $\Sigma$ . By the proof of Theorem 1.1 in (Ghashami et al., 2016), we have

$$\begin{aligned} \rho_{1:T} & \leq \min_{k < \ell} \frac{\|H_T - H_{T,k}\|_F^2}{\ell - k} = \min_{k < \ell} \frac{\sum_{i=k+1}^d \lambda_i(H_T^\top H_T)}{\ell - k} \\ & = \min_{k < \ell} \frac{\sum_{i=k+1}^d \lambda_i(G_T)}{\ell - k} \\ & \leq \sum_{i=\ell}^d \lambda_i(G_T), \end{aligned}$$

where the last inequality follows by choosing  $k = \ell - 1$ .  $\square$

### A.3. Proof details for Section 4.2, S-Shampoo

#### A.3.1. PROOF OF THEOREM 5

*Proof.* First, we establish the following observation and lemma analogous to Observation 7 and Lemma 8:

**Observation 11** (Analogous to Observation 7). *Let  $V_t \Sigma_t^L V_t^\top = \bar{L}_{t-1} + G_t G_t^\top$  be the eigendecomposition of the un-deflated sketch, where  $V_t \in \mathbb{R}^{m \times m}$ . Suppose  $\text{rank}(\Sigma_t^L) = k$ , where  $k \in [\ell - 1, \ell - 1 + r]$ . Write  $V_t = [V_t^{\parallel} \ V_t^{\perp}]$ , where  $V_t^{\parallel}$  contain the first  $k$  columns of  $V_t$ . Then by definition*

$$\bar{L}_t + \rho_t^L I \succeq \bar{L}_{t-1} + G_t G_t^\top + \rho_t^L V_t^{\perp} (V_t^{\perp})^\top.$$

Analogously for the right conditioner, let  $W_t \Sigma_t^R W_t^\top = \bar{R}_{t-1} + G_t^\top G_t$ , and write  $W_t = [W_t^{\parallel} \ W_t^{\perp}]$ , then

$$\bar{R}_t + \rho_t^R I \succeq \bar{R}_{t-1} + G_t^\top G_t + \rho_t^R W_t^{\perp} (W_t^{\perp})^\top.$$

**Lemma 12.** (Analogous to Lemma 8) Define  $N_t^L = V_t^\perp (V_t^\perp)^\top, N_t^R = W_t^\perp (W_t^\perp)^\top$ , then

$$\begin{aligned}\tilde{L}_t &\succeq \sum_{s=1}^t G_s G_s^\top + \sum_{s=1}^t \rho_s^L N_s^L + \varepsilon I_m, \\ \tilde{R}_t &\succeq \sum_{s=1}^t G_s^\top G_s + \sum_{s=1}^t \rho_s^R N_s^R + \varepsilon I_n.\end{aligned}$$

We follow the shampoo proof in (Gupta et al., 2018). Let  $x_t = \overline{\text{vec}}(X_t)$ ,  $g_t = \overline{\text{vec}}(G_t)$ , where  $\overline{\text{vec}}(\cdot)$  denote the row-major vectorization of a given matrix.

Kronecker product  $\otimes$  obeys the following properties as shown in (Gupta et al., 2018):

**Lemma 13** (Lemma 3,4 in Gupta et al. (2018)). *For matrices  $A, A', B, B'$  of appropriate dimensions and vectors  $u, v, L \in \mathbb{R}^{m \times m}, R \in \mathbb{R}^{n \times n}, G \in \mathbb{R}^{m \times n}$ , the following properties hold:*

1.  $(A \otimes B)(A' \otimes B') = (AA') \otimes (BB')$ .
2.  $(A \otimes B)^\top = A^\top \otimes B^\top$ .
3.  $A, B \succeq 0, (A \otimes B)^{-1} = A^{-1} \otimes B^{-1}$ .
4.  $A \succeq A', B \succeq B', \text{ then } A \otimes B \succeq A' \otimes B'$ .
5.  $\text{tr}(A \otimes B) = \text{tr}(A) + \text{tr}(B)$ .
6.  $\overline{\text{vec}}(uv^\top) = u \otimes v$ .
7.  $(L \otimes R^\top)\overline{\text{vec}}(G) = \overline{\text{vec}}(LGR)$ .

Then the shampoo update is

$$x_{t+1} = x_t - \eta(\tilde{L}_t^{1/4} \otimes \tilde{R}_t^{1/4})^{-1} g_t.$$

Let  $\tilde{H}_t \stackrel{\text{def}}{=} \tilde{L}_t^{1/4} \otimes \tilde{R}_t^{1/4}$ , then by Lemma 13,  $\tilde{H}_t$  is monotone increasing with  $t$ , since  $\tilde{L}_t$  and  $\tilde{R}_t$  are monotone by Observation 11. Thus, by standard analysis (Hazan et al., 2016) for Online Mirror Descent (OMD), we can break down the regret into the diameter bound and the gradient bound:

$$\text{Regret}_T \leq R_D + R_G, \quad \text{where}$$

$$\begin{aligned}R_D &= \frac{1}{2\eta} \sum_{t=1}^T \left( \|x_t - x^*\|_{\tilde{H}_t}^2 - \|x_{t+1} - x^*\|_{\tilde{H}_t}^2 \right), \\ R_G &= \frac{\eta}{2} \sum_{t=1}^T \left( \|g_t\|_{\tilde{H}_t}^*\right)^2.\end{aligned}$$

We proceed to bound  $R_D$  and  $R_G$  separately. For  $R_D$ ,

$$\begin{aligned}R_D &\leq \frac{1}{2\eta} \sum_{t=1}^T \|x_t - x^*\|_{\tilde{H}_t - \tilde{H}_{t-1}}^2 + \|x_1 - x^*\|_{\tilde{H}_0}^2 \\ &\leq \frac{1}{2\eta} \sum_{t=1}^T \|\tilde{H}_t - \tilde{H}_{t-1}\|_{\text{op}} \|x_t - x^*\|_2^2 + \|x_1 - x^*\|_{\tilde{H}_0}^2 \\ &\leq \frac{D^2}{2\eta} \sum_{t=1}^T \text{tr}(\tilde{H}_t - \tilde{H}_{t-1}) + \|x_1 - x^*\|_{\tilde{H}_0}^2 \\ &\leq \frac{D^2}{2\eta} \text{tr}(\tilde{H}_T),\end{aligned}$$

where  $\leq_1$  holds since  $\tilde{H}_t$ 's are increasing in  $t$ , and we have for positive semidefinite matrices  $\text{tr}(\cdot) \geq \|\cdot\|_{\text{op}}$ .

Now we try to bound  $R_G$ . First, we have that

**Lemma 14** (Lemma 8 in Gupta et al. (2018)). *If  $G \in \mathbb{R}^{m \times n}$  with rank at most  $r$ , and  $g = \overline{\text{vec}}(G)$ , then  $\forall \varepsilon \geq 0, \forall t$ ,*

$$\begin{aligned}\varepsilon I_{mn} + \frac{1}{r} \sum_{s=1}^t g_s g_s^\top &\preceq \left( \varepsilon I_m + \sum_{s=1}^t G_s G_s^\top \right)^{1/2} \\ &\quad \otimes \left( \varepsilon I_n + \sum_{s=1}^t G_s^\top G_s \right)^{1/2}.\end{aligned}$$

Define  $M_t^L \in \mathbb{R}^{m \times m}, M_t^R \in \mathbb{R}^{n \times n}$  by

$$\begin{aligned}M_t^L &\stackrel{\text{def}}{=} \sum_{s=1}^t G_s G_s^\top + \sum_{s=1}^t \rho_s^L N_s^L + \varepsilon I_m, \\ M_t^R &\stackrel{\text{def}}{=} \sum_{s=1}^t G_s^\top G_s + \sum_{s=1}^t \rho_s^R N_s^R + \varepsilon I_n,\end{aligned}$$

then by Lemma 12,

$$\tilde{L}_t \succeq M_t^L, \quad \tilde{R}_t \succeq M_t^R.$$

Observe that in addition,

$$M_t^L \succeq \varepsilon I_m + \sum_{s=1}^t G_s G_s^\top, \quad M_t^R \succeq \varepsilon I_n + \sum_{s=1}^t G_s^\top G_s.$$

Again by Lemma 13,

$$\begin{aligned}I_m \otimes \left( \varepsilon I_n + \sum_{s=1}^t G_s^\top G_s \right) &\preceq I_m \otimes M_t^R, \\ \left( \varepsilon I_m + \sum_{s=1}^t G_s G_s^\top \right) \otimes I_n &\preceq M_t^L \otimes I_n.\end{aligned}$$

Combining, we have

$$\begin{aligned} \varepsilon I_{mn} + \frac{1}{r} \sum_{s=1}^t g_s g_s^\top &\preceq (M_t^L)^{1/2} \otimes (M_t^R)^{1/2} \\ &\preceq \tilde{L}_t^{1/2} \otimes \tilde{R}_t^{1/2}. \end{aligned}$$

Define  $\hat{H}_t \succ 0 \forall t \in [T]$  by

$$\hat{H}_t \stackrel{\text{def}}{=} \left( r\varepsilon I_{mn} + \sum_{s=1}^t g_s g_s^\top \right)^{1/2} \preceq \sqrt{r} \tilde{H}_t.$$

The bound on  $R_G$  depends on the following lemma:

**Lemma 15** (Lemma 2 in Gupta et al. (2018)). *Consider a sequence of vectors  $\{g_t\}_{t=1}^T$ . Given a function  $\Phi(\cdot)$  over positive semidefinite matrices,*

$$\sum_{t=1}^T (\|g_t\|_{H_t}^*)^2 \leq \sum_{t=1}^T (\|g_t\|_{H_T}^*)^2 + \Phi(H_T) - \Phi(H_0),$$

where

$$H_t = \underset{H \succ 0}{\operatorname{argmin}} \left\{ \left( \sum_{s=1}^t g_s g_s^\top \right) \cdot H^{-1} + \Phi(H) \right\}.$$

Let  $\Phi(H) \stackrel{\text{def}}{=} \operatorname{tr}(H) + r\varepsilon \operatorname{tr}(H^{-1})$  and since

$$\begin{aligned} &\underset{H \succ 0}{\operatorname{argmin}} \left\{ \left( \sum_{s=1}^t g_s g_s^\top \right) \cdot H^{-1} + \Phi(H) \right\} \\ &= \underset{H \succ 0}{\operatorname{argmin}} \left\{ \operatorname{tr}(\hat{H}_t^2 H^{-1} + H) \right\} = \hat{H}_t, \end{aligned}$$

the above lemma gives

$$\begin{aligned} \sum_{t=1}^T (\|g_t\|_{\hat{H}_t}^*)^2 &\leq \sum_{t=1}^T (\|g_t\|_{\hat{H}_T}^*)^2 + \Phi(\hat{H}_T) - \Phi(\hat{H}_0) \\ &\leq 2 \operatorname{tr}(\hat{H}_T), \end{aligned}$$

which by inequality of  $\hat{H}_t$  and  $\tilde{H}_t$  established above, gives

$$\begin{aligned} R_G &\stackrel{\text{def}}{=} \frac{\eta}{2} \sum_{t=1}^T (\|g_t\|_{\tilde{H}_t}^*)^2 \leq \frac{\eta\sqrt{r}}{2} \sum_{t=1}^T (\|g_t\|_{\tilde{H}_t}^*)^2 \\ &\leq \eta\sqrt{r} \operatorname{tr}(\hat{H}_T) \leq \eta r \operatorname{tr}(\tilde{H}_T). \end{aligned}$$

Combining the bound on  $R_D$  and  $R_G$ , the overall regret is

$$\begin{aligned} \operatorname{Regret}_T &\leq R_D + R_G \leq \left( \frac{D^2}{2\eta} + \eta r \right) \operatorname{tr}(\tilde{H}_T) \\ &= \sqrt{2r} D \operatorname{tr}(\tilde{H}_T) = \sqrt{2r} D \operatorname{tr}(\tilde{L}_T^{1/4}) \operatorname{tr}(\tilde{R}_T^{1/4}). \end{aligned}$$

by the choice of  $\eta = \frac{D}{\sqrt{2r}}$  and trace multiplicative equality in Lemma 13. Finally, we have

$$\begin{aligned} \operatorname{tr}(\tilde{L}_T^{1/4}) &\leq_1 \operatorname{tr}(\bar{L}_T^{1/4}) + \operatorname{tr}((\rho_{1:T}^L I_m)^{1/4}) \\ &\leq_2 \operatorname{tr}\left(\left(\sum_{t=1}^T G_t G_t^\top + \varepsilon I\right)^{1/4}\right) + m (\rho_{1:T}^L)^{1/4} \\ &= \operatorname{tr}(L_T^{1/4}) + m (\rho_{1:T}^L)^{1/4}, \end{aligned}$$

where  $\leq_1$  follows from definition of  $\tilde{L}_T$  in Algorithm 3 and subadditivity of  $\operatorname{tr}((\cdot)^{1/4})$  (Audenaert, 2014),  $\leq_2$  follows from Remark 9. Similarly,

$$\operatorname{tr}(\tilde{R}_T^{1/4}) \leq \operatorname{tr}(R_T^{1/4}) + n (\rho_{1:T}^R)^{1/4}.$$

□

### A.3.2. PROOF OF LEMMA 12

*Proof.* We will show the first inequality as the second inequality holds analogously. For  $t = 0$ ,  $\tilde{L}_0 = \varepsilon I_m$  by definition of algorithm. Suppose the first inequality holds for  $t$ . Consider  $t + 1$ :

$$\begin{aligned} \tilde{L}_{t+1} &= \bar{L}_{t+1} + \rho_{1:t+1}^L I_m \\ &\succeq_1 \bar{L}_t + G_{t+1} G_{t+1}^\top + \rho_{t+1}^L N_{t+1} + \rho_{1:t}^L I_m \\ &= \tilde{L}_t + G_{t+1} G_{t+1}^\top + \rho_{t+1}^L N_{t+1} \\ &\succeq_2 \sum_{s=1}^{t+1} G_s G_s^\top + \sum_{s=1}^{t+1} \rho_s^L N_s^L + \varepsilon I_m, \end{aligned}$$

where  $\succeq_1$  follows from Observation 11 and  $\succeq_2$  follows from induction hypothesis. □

## B. Architecture Settings

Neural net architecture settings are taken from the default settings of the `init2winit` library at hash `e337ffe` (Gilmer et al., 2021), which reference the MLCommons specifications provided at MLCommons® open engineering consortium (2023), including the MLPerf ResNet-50 variant (Reddi et al., 2019), Conformer, and GNN. The Distributed Shampoo implementation was run at hash `83e6e62` in the repository referenced by Anil et al. (2020).

We requested a Shampoo tuning script from Dayma & Anil (2022); Anil et al. (2020), which fixed several parameters for Shampoo outside the usual defaults. We tuned on a cluster of TPUv3s.

- Block size was already set to 1024. As mentioned in Sec. 5.1, we kept this change for consistency in covariance factor size across architectures.
- Preconditioning was set to start 101 steps into training (`start_preconditioning_step`).
- Preconditioners were updated every 10 steps instead of every step for speed (`preconditioning_compute_steps` is 10).
- The grafting type, which controls the per-tensor learning rate schedule, was set to `RMSPROP_NORMALIZED`, which applies RMSProp (Hinton et al., 2012) over unit-normalized gradients.
- `moving_average_for_momentum` was activated (so the final updates are computed as  $\beta_1 \mu_t + (1 - \beta_1)g_t$ , where  $\mu_t$  is the momentum term and  $g_t$  is the preconditioned update).
- The virtual batch size, used to compute batch norm statistics, was set to 32 (the full per-step minibatch size was 1024, but this enables data-parallel training).

Also from the provided script, we used a linear warmup rampup starting from 0 to the nominal learning rate hyperparameter setting, followed by a cosine decay schedule, with the transition happening 5% of the way into training (the learning rate monotonically increases, then monotonically decreases, as the cosine schedule has a quarter-period set to the number of training steps).

Then, we performed tuning using random hyperparameter search over the space defined in Tbl. 3. We ran the batch sizes and number of steps provided in the scripts, which were 256, 512, 1024 for Conformer, GNN, and ResNet-50, respectively, for about 162, 117, 199 epochs, respectively.

Shampoo is automatically configured with grafting parameters, which we search over (Agarwal et al., 2020).

Table 3: The search space for hyperparameters for tuning Shampoo on our NN architectures for the Kronecker-factored covariance optimization. Note that the search space explores one less momentum, not momentum directly. Label smoothing was only applied to ImageNet. We sample uniformly either from linear or logscale among the ranges specified with 100 trials, and select the best one according to validation accuracy.

Hyperparameter	Range	Log scale?
Learning rate $\eta$	$[10^{-4}, 10^{-2}]$	✓
Weight decay $\gamma$	$[10^{-2}, 1]$	✓
Momentum $1 - \beta_1$	$[10^{-2}, 10^{-1}]$	✓
Label smoothing	$[0, 0.2]$	

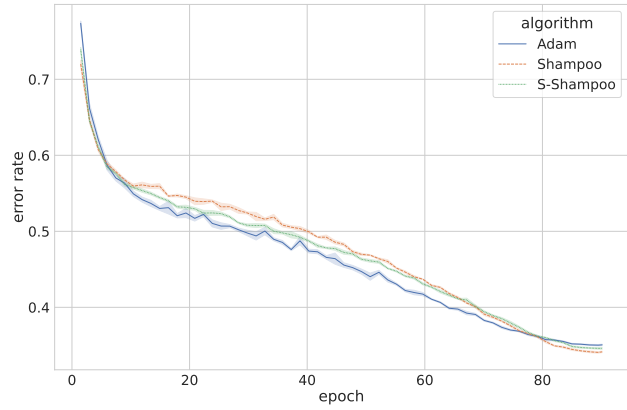


Figure 6: Full test set curves for imagenet.

## C. ResNet-50 Settings

For training ImageNet, we mostly inherited the settings of Appendix B for Shampoo tuning, but made some minor modifications, namely adding of the second moment decay ( $\beta_2$ ), widening the search space, and, for computational reasons, performing a shortened run of only 66 epochs for tuning trials. The architecture details remain the same. The learning rate schedule was stretched to this interval, so warmup was still 5% of the duration, and cosine decay ended learning rate at 0 by the end of the 66 epochs of training. The full search space is elaborated on in Tbl. 4.

To tune Adam, a first order method, we considered mostly the same nominally hyperparameters (where  $\beta_2$  refers to second moment momentum now), except grafting, which instead we replaced with a search over the warmup duration, summarized in Tbl. 5.

Full evaluation of the selected best hyperparameters for each setting was performed with the classical 90-epoch setting, with the learning rate schedule correspondingly stretched.

We provide the full training curves in Fig. 6.

Table 4: The search space for hyperparameters for tuning Shampoo on our architectures for ImageNet hyperparameters. The same space was applied to S-Shampoo with a fixed sketch rank  $\ell = 256$  for all tensors. Note that we search  $1 - \beta_1, 1 - \beta_2$ , and not the original hyperparameter. We sample uniformly either from linear or logscale among the ranges specified with 256 trials, and select the best one according to validation accuracy. (\*) stands for a discrete uniform choice over four different grafting rates, based on AdaGrad, RMSProp, and normalized versions of the two. The gradient clipping norm is similarly discrete.

Hyperparameter	Range	Log?
Learning rate $\eta$	$[10^{-4}, 10^{-2}]$	✓
Weight decay $\gamma$	$[10^{-3}, 0.1]$	✓
Momentum $1 - \beta_1$	$[10^{-4}, 10^{-1}]$	✓
$2^{\text{nd}}$ moment $1 - \beta_2$	$[10^{-4}, 10^{-1}]$	✓
Label smoothing	$[0, 0.2]$	
Dropout Rate	$[0, 0.2]$	
Grafting Type	(*)	
Gradient Clip $L_2$	$\{1, 10, 10^2, 10^3\}$	

Table 5: The search space for hyperparameters for tuning Adam on our architectures for ImageNet hyperparameters. The same caveats as in Tbl. 4 apply. Also tuned with 256 trials.

Hyperparameter	Range	Log?
Learning rate $\eta$	$[10^{-4}, 10^{-2}]$	✓
Weight decay $\gamma$	$[10^{-3}, 0.1]$	✓
Momentum $1 - \beta_1$	$[10^{-4}, 10^{-1}]$	✓
$2^{\text{nd}}$ moment $1 - \beta_2$	$[10^{-4}, 10^{-1}]$	✓
Label smoothing	$[0, 0.2]$	
Dropout Rate	$[0, 0.2]$	
Warmup Duration	$[2\%, 10\%]$ of training	
Gradient Clip $L_2$	$\{1, 10, 10^2, 10^3\}$	

Table 6: The search space for hyperparameters for tuning Shampoo, Adam, and S-Shampoo for Conformer with fixed 256 rank. Here we fixed the grafting type to be RMSProp. During initial runs of the baselines, we noticed that Adam preferred larger learning rates, so we changed and reran its space for  $\eta$  to be  $10 \times$  that of Shampoo, namely  $[10^{-4}, 10^{-2}]$ , still searching over logspace. We also stopped any hyperparameter trial which did not go below 0.875 WER after 5000 training steps.

Hyperparameter	Range	Log?
Learning rate $\eta$	$[10^{-5}, 10^{-3}]$	✓
Momentum $1 - \beta_1$	$[10^{-3}, 10^{-1}]$	✓
$2^{\text{nd}}$ moment $1 - \beta_2$	$[10^{-3}, 10^{-1}]$	✓
Weight decay $\gamma$	$[10^{-4}, 10^{-2}]$	✓
Dropout Rate	$[0, 0.2]$	✓

## D. Conformer Settings

The Conformer architecture was used from the MLCommons specification as described in Appendix B, with the following fixed additional settings: 1024 batch size, 100 epochs of training, 5% of training used for linear warmup with cosine decay of learning rate. We fixed gradient clipping at a value of 10, without which we noticed Adam curves were very volatile. We set the `eigh` parameter for Shampoo to true (we found that it did not make a difference in a few sample runs’ loss curves, as an alternative to the iterative  $p$ -th inverse root routine in Shampoo, but used it instead since we believe it has better numerical stability). The hyperparameters we searched over for all optimizers are described in Tbl. 6.

## E. GNN Settings

To evaluate the many GNN settings with fixed regularization parameters, we ran smaller hyperparameter tunings for each different rank.

The GNN architecture was used from the MLCommons specification as described in Appendix B, with the following fixed additional settings: 1024 batch size, 50 epochs of training, 5% of training used for linear warmup with cosine decay of learning rate, a fixed 0.01 weight decay (treated as direct weight decay, not Euclidean norm loss), 0.1 dropout, and we set the `eigh` parameter for Shampoo to true as in Appendix D.

Then we searched a reduced hyperparameter space fixed for Shampoo and S-Shampoo as described in Tbl. 7.

Table 7: The search space for hyperparameters for tuning Shampoo and S-Shampoo for GNN with fixed regularization settings (across ranks  $\ell = 32, 64, 128$ ). Here we fixed the grafting type to be RMSProp and did not use gradient clipping, unlike Tbl. 4, based on a few trial runs of the Shampoo baseline from which we determined we could reduce the hyperparameter space. Due to the need for more curves, and computational demand, we only ran 16 random trials over this smaller space.

Hyperparameter	Range	Log?
Learning rate $\eta$	$[10^{-4}, 10^{-2}]$	✓
Momentum $1 - \beta_1$	$[10^{-3}, 0.5]$	✓
$2^{\text{nd}}$ moment $1 - \beta_2$	$[10^{-3}, 0.5]$	✓

## F. Step-skipping

In this section, we provide some theoretical justification for step-skipping. We first derive the regret bound of AdaGrad with step skipping, named Generic Epoch AdaGrad. The additional regret incurred is expressed as an error term. Then, we describe a setting where the error term admits a simple bound, showing that step-skipping incurs at most an extra  $\log T$  time dependence on the regret.

### F.1. Adversarial losses

Consider a generalized epoching AdaGrad with  $K$  fixed update points  $t_k$ , such that  $t_1 = 0$  and  $t_K = T$ .

---

#### Algorithm 4 Generic Epoch AdaGrad

---

```

1: Input:  $\eta, T, \{t_k\}_{k=1}^K, G_0 \succ 0$ , convex closed set  $\mathcal{K}$ .
2: Initialize:  $x_1$ .
3: for  $k = 1, \dots, K - 1$  do
4:   for  $t = t_k + 1, \dots, t_{k+1}$  do
5:     Play  $x_t$ , receive  $f_t$  loss with gradient  $g_t$ .
6:     Update  $G_t = G_{t-1} + g_t g_t^\top$ .
7:     Update  $x_{t+1} = \Pi_{\mathcal{K}}[x_t - \eta G_{t_k}^{-1/2} g_t]$ .
8:   end for
9: end for

```

---

**Theorem 16.** *Generic Epoch AdaGrad (Alg. 4) with fixed update points  $\{t_k\}_{k=1}^K$  satisfies*

$$R_T \leq \frac{D^2}{\eta} \operatorname{tr} G_T^{1/2} + \frac{\eta}{2} \left( 2 \operatorname{tr} G_T^{1/2} - 2 \operatorname{tr} G_0^{1/2} + \sum_{k=1}^K \epsilon_k \right) ,$$

where the error terms  $\epsilon_k$  are given by

$$\begin{aligned} \epsilon_k &= \operatorname{tr} \left( G_{t_k}^{-1/2} S_k G_{t_k}^{-1/2} A_k \right) , \\ S_k &= \int_0^\infty \exp \left( -\tau G_{t_k}^{1/2} \right) A_k \exp \left( -\tau G_{t_k}^{1/2} \right) d\tau , \\ A_k &= G_{t_{k+1}} - G_{t_k} . \end{aligned}$$

*Proof of Theorem 16.* First we start with the usual decomposition.

**Lemma 17.** *Consider arbitrary adversarial convex losses  $f_t$ . Without projection, the regret  $R_T$  relative to a comparator  $x_*$  with  $D = \max_t \|x_t - x_*\|_2$ , for generic epoch AdaGrad with fixed update points  $t_k$  is given by*

$$R_T \leq \frac{D^2}{\eta} \operatorname{tr} G_T^{1/2} + \frac{\eta}{2} \sum_{k=1}^K \sum_{t=t_k+1}^{t_{k+1}} g_t^\top G_{t_k}^{-1/2} g_t .$$

*Proof of Lemma 17.* This follows from the usual AdaGrad analysis since our preconditioners are monotone  $G_{t_k} \succeq G_{t_{k+1}}$ .  $\square$

So we must turn our attention to the gradient bound. We start by noting the following lemmas established in matrix analysis.

**Lemma 18** (Corollary 4.1 in (Ando, 1979)). *The map  $f(X) = X^{-1/2}$  is matrix convex over the positive definite domain; i.e., for any two matrices  $A, B \succ 0$  and any  $\theta \in [0, 1]$ , we have*

$$\theta f(A) + (1 - \theta) f(B) \succeq f(\theta A + (1 - \theta)B) .$$

**Lemma 19** (Theorem V.3.3, Exercise V.3.15 in (Bhatia, 1997)). *Suppose a matrix convex function  $F(X)$  is induced by applying  $f$  pointwise to its spectrum  $F(X) = U \operatorname{diag}[f(\Lambda_{ii})] U^\dagger$  with  $f \in \mathcal{C}^1(I)$  for some  $I \subset \mathbb{R}_+$ . Then*

$$F(X) + \partial F(X)(\Delta) \preceq F(X + \Delta) ,$$

*if and only if  $F(X)$  is matrix convex, and the linear transformation  $\partial F(X)$  is the derivative of  $F$  at  $X$ .*

Matrix derivative computation (Petersen et al., 2008; Brockett, 2015) shows that if  $F(X) = X^{-1/2}$  then

$$\partial F(X)(\Delta) = -X^{-1/2} \left[ (X^{1/2} \oplus X^{1/2})^{-1} \Delta \right] X^{-1/2} ,$$

where  $(X^{1/2} \oplus X^{1/2})^{-1} \Delta$  is the solution  $S$  to the continuous Lyapunov equation  $\sqrt{X}S + S\sqrt{X} = \Delta$  as  $X \oplus X = I \otimes X + X \otimes I$ . For  $X \succ 0$ , it is known from generic results about Sylvester's equation that the solution  $S$  is unique. Since  $-X$  is asymptotically stable in the Lyapunov sense,

$$S(X, \Delta) = \int_0^\infty \exp(-\tau \sqrt{X}) \Delta \exp(-\tau \sqrt{X}) d\tau .$$

With these results from matrix analysis and linear systems, we are ready to bound the gradient term in Lemma 17. Consider a single term from the gradient bound in Lemma 17,  $\sum_{t=t_k+1}^{t_{k+1}} g_t^\top G_{t_k}^{-1/2} g_t$  for fixed  $k$ .

With  $X = G_{t_k}$ ,  $\Delta = A_k = G_{t_{k+1}} - G_{t_k}$ , and  $f(X) = X^{-1/2}$  consider applying Lemma 19.  $F(X) \preceq F(X +$

$A_k) - \partial F(X)(A_k)$ , so overall

$$\begin{aligned}
 & \sum_{t=t_k+1}^{t_{k+1}} g_t^\top G_{t_k}^{-1/2} g_t \\
 & \leq \sum_{t=t_k+1}^{t_{k+1}} g_t^\top \left[ G_{t_{k+1}}^{-1/2} - \partial F(G_{t_k})(A_k) \right] g_t \\
 & = \sum_{t=t_k+1}^{t_{k+1}} g_t^\top G_{t_{k+1}}^{-1/2} g_t - \text{tr} \left( \partial F(G_{t_k})(A_k) \sum_{t=t_k+1}^{t_{k+1}} g_t g_t^\top \right) \\
 & = \sum_{t=t_k+1}^{t_{k+1}} g_t^\top G_{t_{k+1}}^{-1/2} g_t - \text{tr} (\partial F(G_{t_k})(A_k) A_k) \\
 & = \sum_{t=t_k+1}^{t_{k+1}} g_t^\top G_{t_{k+1}}^{-1/2} g_t + \text{tr} \left( G_{t_k}^{-1/2} S_k G_{t_k}^{-1/2} A_k \right) \\
 & = \sum_{t=t_k+1}^{t_{k+1}} g_t^\top G_{t_{k+1}}^{-1/2} g_t + \epsilon_k .
 \end{aligned}$$

**Lemma 20** (FTL-BTL with errors). *Consider arbitrary  $\phi_k$  for  $k \in 0, 1, \dots, K$ . Let  $x_k \in \operatorname{argmin} \sum_{j=0}^k \phi_j$  and suppose  $\phi_k(x_{k-1}) \leq \phi_k(x_k) + \delta_k$ . Then  $\forall K$ ,*

$$\sum_{k=0}^K \phi_k(x_{k-1}) \leq \sum_{k=0}^K \phi_k(x_k) + \delta_k ,$$

with  $\delta_0 = 0$  and  $x_{-1} = x_0$ .

Assume Lemma 20 and take  $\phi_k(X) = \langle A_k, X \rangle$  for  $X \succeq 0$  and  $\phi_0(X) = \langle G_0, X \rangle + \text{tr } X^{-1}$ . Note that

$$\sum_{j=0}^k \phi_j(X) = \text{tr } X^{-1} + \sum_{j=0}^k \langle A_j, X \rangle .$$

In particular,  $G_{t_{k+1}}^{-1/2} = \operatorname{argmin}_{X \succeq 0} \sum_{j=0}^k \phi_j(X)$ .

Furthermore, with  $\delta_k = \epsilon_k$ , the condition  $\phi_k(G_{t_k}) \leq \phi_k(G_{t_{k+1}}) + \delta_k$  is satisfied. Lemma 20 implies

$$\begin{aligned}
 & \sum_{k=1}^K \sum_{t=t_k+1}^{t_{k+1}} g_t^\top G_{t_k}^{-1/2} g_t = \sum_{k=1}^{K-1} \phi_k \left( G_{t_k}^{-1/2} \right) \\
 & = -\phi_0 \left( G_0^{-1/2} \right) + \sum_{k=0}^{K-1} \phi_k \left( G_{t_k}^{-1/2} \right) \\
 & \leq -\phi_0 \left( G_0^{-1/2} \right) + \sum_{k=0}^{K-1} \phi_k \left( G_T^{-1/2} \right) + \epsilon_k ,
 \end{aligned}$$

where  $G_{t_0} \stackrel{\text{def}}{=} G_0$ . Lastly, since

$$\begin{aligned}
 \sum_{k=0}^{K-1} \phi_k \left( G_T^{-1/2} \right) & = \text{tr } G_T^{1/2} + \text{tr} \left( G_T^{-1/2} \sum_{k=0}^{K-1} A_k \right) \\
 & = 2 \text{tr } G_T^{1/2} ,
 \end{aligned}$$

we conclude with the desired bound for  $R_T$ .  $\square$

*Proof of Lemma 20.* By induction on  $K$ . For  $K = 0$ ,  $\phi_0(x_{-1}) = \phi_0(x_0)$ , holding by definition. Suppose that the hypothesis now holds for  $K$ ; it then holds for  $K+1$ .

$$\begin{aligned}
 \sum_{k=0}^{K+1} \phi_k(x_{K+1}) & = \sum_{k=0}^K \phi_k(x_{K+1}) + \phi_{K+1}(x_{K+1}) \\
 & \geq \phi_{K+1}(x_{K+1}) + \sum_{k=0}^K \phi_k(x_K) \\
 & \geq \phi_{K+1}(x_K) - \epsilon_{K+1} + \sum_{k=0}^K \phi_k(x_K) \\
 & \geq \phi_{K+1}(x_K) - \epsilon_{K+1} + \sum_{k=0}^K \phi_k(x_{k-1}) - \epsilon_k \\
 & \geq \sum_{k=0}^{K+1} \phi_k(x_{k-1}) - \epsilon_k .
 \end{aligned}$$

## F.2. Simplifying the error

We want to simplify the term  $\epsilon_k$ , which is given by

$$\begin{aligned}
 \epsilon_k & = \text{tr} \left( G_{t_k}^{-1/2} S_k G_{t_k}^{-1/2} A_k \right) , \\
 S_k & = \int_0^\infty \exp \left( -\tau G_{t_k}^{1/2} \right) A_k \exp \left( -\tau G_{t_k}^{1/2} \right) d\tau , \\
 A_k & = G_{t_{k+1}} - G_{t_k} .
 \end{aligned}$$

Next, notice that  $X$  and  $\exp(-\alpha X^{-1})$  commute. Then along with linearity of trace, we can establish that

$$\epsilon_k = \int_0^\infty \text{tr} \left[ \left( \exp \left( -\tau G_{t_k}^{1/2} \right) G_{t_k}^{-1/2} A_k \right)^2 \right] d\tau .$$

## F.3. Towards simpler error

$\epsilon_k$  can be further simplified and bounded under additional assumptions. Namely,

**Assumption 1.** Suppose that w.p. at least  $1 - \delta/2K$  for some fixed, universal  $\beta > 0$ , we have the inequality  $A_k \preceq \beta G_{t_k}$  where  $A_k \stackrel{\text{def}}{=} G_{t_{k+1}} - G_{t_k}$ .

**Assumption 2.** Suppose that w.p. at least  $1 - \delta/2K$ ,  $G_{t_k}$ 's are  $(\sigma_{\min}, \sigma_{\max})$ -well-conditioned, i.e.

$$\lambda_d(G_{t_k}) \geq \sigma_{\min} t_k \quad \text{and} \quad \lambda_1(G_{t_k}) \leq \sigma_{\max} t_k .$$

**Remark 21.** As an example, consider the stochastic linear setting where at each iteration we receive a loss function  $\langle g_t, x \rangle$ , and  $g_t$ 's are independent, though not necessarily identically distributed, and satisfies that  $2\sigma_{\min} I \preceq$

$\mathbb{E}[g_t g_t^\top] \preceq \frac{\sigma_{\max}}{2} I$  and  $\|g_t\|_2 \leq \sqrt{\frac{\sigma_{\max}}{2}}$  almost surely. Then, for  $T$  sufficiently large and  $t_{k+1} - t_k = O(\log T)$ , by matrix Chernoff bounds Assumption 1 and 2 are satisfied.

First,  $\forall X, Y \succeq 0$ , the following inequality hold:

**Lemma 22.** *If  $X \preceq Y$  and  $A \succeq 0$ , then  $\text{tr}[(AX)^2] \leq \text{tr}[(AY)^2]$ .*

With Lemma 22, we can bound  $\epsilon_k$ . With probability at least  $1 - \delta/2K$ ,

$$\begin{aligned} \epsilon_k &= \int_0^\infty \text{tr} \left[ \left( \exp \left( -\tau G_{t_k}^{1/2} \right) G_{t_k}^{-1/2} A_k \right)^2 \right] d\tau \\ &\leq \beta^2 \int_0^\infty \text{tr} \left[ \left( \exp \left( -\tau G_{t_k}^{1/2} \right) G_{t_k}^{-1/2} G_{t_k} \right)^2 \right] d\tau \\ &= \beta^2 \int_0^\infty \text{tr} \left[ \left( \exp \left( -\tau G_{t_k}^{1/2} \right) G_{t_k}^{1/2} \right)^2 \right] d\tau \\ &= \beta^2 \int_0^\infty \text{tr} \left( \exp \left( -2\tau G_{t_k}^{1/2} \right) G_{t_k} \right) d\tau, \end{aligned}$$

where the last step only holds since  $X$  and  $\exp(-\alpha X^{-1/2})$  commute.

Next, let  $\lambda_i$  denote the  $i$ -th largest eigenvalue and  $\lambda_{-i}$  be the  $i$ -th smallest. Notice since  $\exp(-\tau G_{t_k}^{1/2})$ ,  $G_{t_k}^{1/2}$ , and  $G_{t_k}$  are simultaneously diagonalizable, and monotonic matrix functions preserve eigenvalue ordering, we have

$$\begin{aligned} \lambda_i \left( \exp \left( -2\tau G_{t_k}^{1/2} \right) \right) &= \exp \left( -2\tau \lambda_{-i} \left( (G_{t_k})^{1/2} \right) \right), \\ \lambda_i \left( \exp \left( -2\tau G_{t_k}^{1/2} \right) G_{t_k} \right) &= \lambda_i \left( \exp \left( -2\tau G_{t_k}^{1/2} \right) \right) \lambda_i(G_{t_k}) \end{aligned}$$

Returning to our  $\epsilon_k$  bound, rewriting the trace with eigenvalues, we have w.p. at least  $1 - \delta/2K$ ,

$$\begin{aligned} \epsilon_k &\stackrel{1}{\leq} \beta^2 \int_0^\infty \sum_i \lambda_i \left( \exp \left( -2\tau G_{t_k}^{1/2} \right) G_{t_k} \right) d\tau \\ &= \beta^2 \sum_i \lambda_i(G_{t_k}) \int_0^\infty \exp \left( -2\tau \lambda_{-i}(G_{t_k})^{1/2} \right) d\tau \\ &= \beta^2 \sum_i \frac{\lambda_i(G_{t_k})}{2\lambda_{-i}(G_{t_k})^{1/2}}, \end{aligned}$$

where  $\leq_1$  follows from Tonelli's Theorem. At this point,

we apply Assumption 2 and get that w.p. at least  $1 - \delta/K$ ,

$$\begin{aligned} \epsilon_k &\leq \frac{\beta^2}{\sqrt{t_k \sigma_{\min}}} \sum_i \lambda_i(G_{t_k}) \\ &\leq \frac{\beta^2}{\sqrt{t_k \sigma_{\min}}} \sum_i (t_k \sigma_{\max})^{1/2} \lambda_i(G_{t_k})^{1/2} \\ &= \beta^2 \sqrt{\frac{\sigma_{\max}}{\sigma_{\min}}} \sum_i \lambda_i(G_{t_k})^{1/2} \\ &= \beta^2 \sqrt{\frac{\sigma_{\max}}{\sigma_{\min}}} \text{tr} G_{t_k}^{1/2}. \end{aligned}$$

Across all epochs, we then have w.p. at least  $1 - \delta$ ,

$$\frac{1}{\beta^2} \sqrt{\frac{\sigma_{\min}}{\sigma_{\max}}} \sum_{k=1}^K \epsilon_k \leq \sum_{k=1}^K \text{tr} G_{t_k}^{1/2} \leq \log T \text{tr} G_T^{1/2}.$$

Altogether, since  $\beta$  is a universal constant, w.p. at least  $1 - \delta$ ,

$$R_T \lesssim \frac{D^2}{\eta} \text{tr} G_T^{1/2} + \eta \sqrt{\frac{\sigma_{\max}}{\sigma_{\min}}} \log T \text{tr} G_T^{1/2}.$$

We conclude that in this case, the time dependency of Epoch AdaGrad's regret is only  $\log T$  factor worse than that of the original AdaGrad regret.

### F.3.1. PROOF OF LEMMA 22

First, for  $0 \preceq X \preceq Y$ ,  $BXB \preceq BYB$ ,  $\forall B$ , since  $(Bx)^\top (Y - X)(Bx) \geq 0$ ,  $\forall x$ . By cyclic property of trace and taking  $B = A^{1/2}X$ ,

$$\begin{aligned} \text{tr}(AXAX) &= \text{tr} \left( X^{1/2} AXAX^{1/2} \right) \\ &\leq \text{tr} \left( X^{1/2} AYAX^{1/2} \right). \end{aligned}$$

$$\begin{aligned} \text{tr}[(AX)^2] &\leq \text{tr} \left( X^{1/2} AYAX^{1/2} \right) \\ &= \text{tr} \left( Y^{1/2} AXAY^{1/2} \right) \\ &\leq \text{tr} \left( Y^{1/2} AYAY^{1/2} \right) \\ &= \text{tr}[(AY)^2]. \end{aligned}$$